

A
Major Project
On

**RADIO OVER FIBER SYSTEMS: EFFECT OF LASER
AND RF OSCILLATOR PHASE NOISES ON THE
PERFORMANCE OF QAM SYSTEMS**

Submitted in the partial fulfillment of the requirement
for the award of the degree of

MASTER OF ENGINEERING
(Electronics & Communication Engineering)

Submitted By

Dharmendra Singh Rana

College Roll No: 02/E&C/05

University Roll No. 2801

Under the Guidance of:

Dr. R. K. Sinha

Applied Physics Department



**DEPARTMENT OF COMPUTER ENGINEERING
DELHI COLLEGE OF ENGINEERING
DELHI UNIVERSITY
2005-2007**

CERTIFICATE

This is to certify that the work contained in this dissertation entitled “**Radio over Fiber Systems: Effect of Laser and RF Oscillator Phase Noises on the Performance of QAM Systems** ” by **Dharmendra Singh Rana** in the requirement for the partial fulfillment for the award of the degree of **Master of Engineering** in Electronics and Communication Engineering, Delhi College of Engineering is an account of his work carried out under my guidance in the academic year 2006-2007.

This work embodied in this dissertation has not been submitted for the award of any other degree to the best of my knowledge.

Dr. R.K.Sinha

Prf. Asok Bhattacharrya

(Project guide)

Head TIFAC Center

H.O.D

Department of Applied Physics

Department of Electronics& communication

Delhi College Of Engineering,

Delhi College Of Engineering,

University of Delhi, Delhi

University of Delhi, Delhi

ACKNOWLEDGEMENT

It is a great pleasure to have the opportunity to extend my heartiest felt gratitude to everybody who helped me throughout the course of this project.

It is distinct pleasure to express my deep sense of gratitude and indebtedness to my learned supervisor Dr. R K Sinha for his invaluable guidance, encouragement and patient reviews. His continuous inspiration only has made me complete this dissertation. He kept on boosting me time and again for putting an extra ounce of effort to realize this work.

I would also like to express my gratitude to Prof. Asok Bhattacharyya for his constant motivation and support.

I would also like to take this opportunity to present my sincere regards to all the faculty members for their support and encouragement.

I am grateful to my parents for their moral support all the time, they have been always around to cheer me up in the odd times of this work. I am also thankful to my classmates for their unconditional support and motivation during this work.

Dharmendra Singh Rana
M.E. (Electronics and Communication)
College Roll No. 02/E&C/05
University Roll No. 2801
Department of Electronics and Communication
Delhi College of Engineering, Delhi-110042

Abstract

The Radio over Fiber systems have of late emerged as the most promising solution for distribution of the radio signals between the base station (BS) and the mobile switching center(MSC) owing to its low cost, reduced complexity at the BS, centralized signal processing and high mobility combined with the high fiber bandwidth low loss over the fiber.

However since the fiber channel is prone to the dispersive effects, any signal launched along the fiber will, due to the dispersive nature of the fiber, have phase noise added to it. This phase noise will affect the performance of the channel and will degrade the Carrier to Noise Ratio (CNR) and hence the Bit error Rate (BER) of the signal launched in the fiber. The phase noises arise due to the finite spectral widths of the laser diode and the RF oscillator.

Further the most promising modulation scheme for the sub carrier modulation (SCM) transmission over the fiber is Qaudrature Amplitude Modulation (QAM) due to its high spectral and power efficiency. The QAM technique combines two Quadrature components of a continuous wave signal and transmits the amplitude and the phase of the signal But one major drawback of the QAM systems is that they are highly sensitive to the both non linearity and the phase noises.

In this thesis we report the effects of the phase noises due to the laser diode and the RF oscillator spectral widths on the BER performance of the 64-QAMRadio over Fiber (RoF) systems. Also the effects of the RF filter bandwidth is studied in detail.

TABLE OF CONTENTS

ABSTRACT

TABLE OF CONTENTS

LIST OF FIGURES

1. RADIO OVER FIBER.....	1
1.1. Introduction.....	1
1.2 What is Radio over Fiber	2
1.2.1. RoF System Architectures	3
1.3. General RoF Architecture	4
1.4. Basic microwave properties of RoF Links.....	13
1.4.1. Insertion Loss.....	15
1.4.2. Noise Figure F.....	16
1.4.4. Bandwidth.....	17
1.4.5. Dynamic Range.....	18
1.5. RoF Architecture for Cellular Networks.....	18
1.6. Advantages of RoF	18
2. APPLICATIONS OF RoF	26
2.1. Introduction.....	26
2.2. Fiber to the Home/Fiber to the Premises(FTTH/FTTP)	28
2.2.1 Fiber access Network Architectures	30
2.2.1.1. Point-to-point architecture	30
2.2.1.2. Active star architecture	30
2.2.1.3. Passive star architecture.....	30
2.3. Radio-over-Fiber Links for Indoor Wireless LANs.....	30
2.4. Radio over Fiber for Beyond 3G and 4G.....	30
2.5. Radio-over-Fiber Network for Microcellular System.....	30
2.6. RoF for Road Vehicle Communication Systems	30
2.7. Radio over Fiber for Mobile Communications.....	30
2.8. Switched RoF Distributed Antenna System (DAS).....	30
2.9. RoF For Ultra Wide Band Radio	30
3. EFFECT OF LASER AND RF OSCILLATOR LINEWIDTHS	32
3.1 Introduction.....	32
3.2. RoF System Architecture.....	32
3.3. CNR Penalty Analysis	33
3.4. Discussion	33
4. 64-QAM RADIO OVER FIBER SYSTEMS.....	39
4.1. Introduction.....	39
4.2. General Architecture of RoF System.....	39
4.3. M-Ary QAM Systems and their BER Performance	40
5. IMPROVEMENT OF SYSTEM BER.....	53
5.1 Introduction.....	53
5.2 BCH) Codes	55

5.3 Code Construction	61
5.4 Architecture of the converter	62
5.4 Decoding	65
6. RESULTS	71
6.1 Uncoded Systems.....	53
6.1.1. Effect of the Laser Linewidth	53
6.1.2 . Effect of the Ratio p.....	53
6.1.3 Effect of the RF Oscillatore Linewidth	53
6.2. Effect of Coding.....	53
7. CONCLUSION	93
7. REFERENCES	93

LIST OF FIGURES

Fig 1.1	IMDD Analog optical link	5
Fig 1.2	Representative RoF link configurations	8
Fig 1.3	Optical heterodyning	9
Fig 1.4	Electroabsorption transceiver (EAT).....	10
Fig 1.5	Schematic illustration of a combination of DWDM and RoF transmission.....	12
Fig 1.6	Optical spectra of DWDM mm-wave RoF signals	12
Fig 1.7	RoF ring architecture based on DWDM.....	13
Fig 1.8	Conceptual drawing of a double-MA wireless network.....	16
Fig. 1.9	. A two-service WDM optical transfer network	16
Fig. 2.1	Point to point architecture	20
Fig. 2.2	Active star architecture	21
Fig. 2.3	Passive Star Architecture.....	22
Fig. 2.4	RoF for Indoor wireless access	24
Fig. 2.5	Evolution of various wireless networks	25
Fig. 2.6	RoF for 3G and 4G.....	26
Fig. 2.7	RoF distribution system with the frequency reuse	28
Fig. 2.8	Block diagram of the fiber-radio link.....	28
Fig. 2.9	A vehicle communication system.....	29
Fig. 2.10	Architecture of the control station and the base station	30
Fig. 2.11	Architecture of a Typical Fiber DAS	31
Fig. 2.12	RoF Architecture for UWB Radio.....	34
Fig. 3.1	Optical link in RoF	38
Fig. 3.2	Δ CNR vs. the percentage of the received power p	45
Fig. 3.3	Δ CNR vs. the laser linewidth	46
Fig. 3.4	Δ CNR vs. the RF linewidth.....	47
Fig. 3.5	Δ CNR vs. RF linewidth expanded view	48
Fig. 3.6	Δ CNR vs. RF linewidth, $L=10$ Km.....	48
Fig. 3.7	Δ CNR vs. RF linewidth, $L=10$ Km expanded view.....	49
Fig. 3.8	Δ CNR vs. RF linewidth, $L=30$ Km.....	49
Fig. 3.9	Δ CNR vs. RF linewidth, $L=30$ Km expanded view.....	50

Fig. 3.10 Δ CNR vs. Chromatic Dispersion D.....	50
Fig. 4.1 General RoF system	57
Fig. 4.2 Constellation Diagram for 64-QAM	58
Fig. 6.1 BER vs. laser linewidth(MHz) for different RF oscillator line width.....	70
Fig. 6.2 BER vs. p for different laser line width.....	71
Fig. 6.3 BER vs. RF oscillator linewidth [Hz]	72
Fig. 6.4 BER versus Laser Linewidth [MHz] for coded case.....	73
Fig. 6.5 BER versus parameter p for coded case.....	74
Fig. 5.11 6 BER versus RF Oscillator Linewidth [Hz] for coded case	75
Fig. 5.11 The action package	76

LIST OF TABLES

Table 5.1 Field of 32 element generated by a polynomial	63
Table 4.1 Decoding of BCH code	66

1. RADIO OVER FIBER

1.1 Introduction

Wireless access fixed or mobile is regarded as an excellent way to achieve broadband services. Of course, it is the only possibility for mobile access (in particular if global mobility is required), however wide application of fixed wireless broadband access is also foreseen. It is well known that both due to unavailability of lower microwave frequencies and the insufficient bandwidth of lower frequency ranges, next generation wireless access systems both mobile and fixed will operate in the upper microwave/millimeter wave frequency band. As in a cellular system both increased traffic and propagation properties of millimeter-waves require small cells, further as millimeter-wave circuits are rather expensive, the cost of base stations (BSs) will be of determining role.

One emerging technology applicable in high capacity, broadband millimeter-wave access systems is Radio over Fiber also called Fiber To The Air (FTTA). In this system – in order to decrease the costs of base stations, most of signal processing (including coding, multiplexing, RF generation & modulation etc) is made in central stations (CS-s) rather than in the BS-s. The signal to and from these is transmitted in the optical band, via a fiber optic network. This architecture makes design of base stations really simple; in the simplest case a BS comprises simply of optical-to-electrical (O/E) and electrical-to-optical (E/O) converters, an antenna and some microwave circuitry (two amplifiers and a diplexer).

1.2. What is Radio over Fiber

Radio over Fiber refers to the transmission of the analog radio signal over the optical fiber link. In an general RoF system a radio frequency carrier is first modulated using digital modulation techniques such as QPSK or QAM. This digitally modulated carrier then modulates the laser light or the supercarrier. This combined signal is then

transmitted over the optical fiber to the remote unit. This technique is advantageous since an optical fiber provides low loss and large bandwidth and a radio signal enables the mobility and easy access.

1.2.1. RoF System Architectures

There are three main radio over fiber system architectures in use in current commercial in-building wireless deployments. All use direct modulation of a laser diode rather than external modulation to reduce cost and complexity. The three types of radio over fiber are;

1. **RF transmission over single mode fiber** directly at the radio carrier frequency (usually in the range 800 - 2200MHz, depending on the radio system). This is the simplest architecture.
2. **IF transmission over multimode or single mode fiber.** The RF signal from the base station is downconverted to IF and transmitted to the remote antennas where it is upconverted back to the original RF. This allows pre-existing multimode Fiber cables to be used, although at the expense of additional cost and complexity.
3. **Digitized IF over multimode or single mode fiber.** This approach uses downconversion to IF as in the previous type and then digitizes the signal for transmission over optical fiber. The analog signal is then re-constructed at IF and converted back to RF. This has the advantages of digital transmission (no impairments due to noise and distortion), but at the expense of even further complexity

The most common of these architectures is the first, RF over single mode fiber, because it is the simplest to design and the lowest cost to implement. However, it places the most stringent requirements on the optical components, which need to have low noise and low distortion at high frequencies. The laser is usually the dominant source of noise and

distortion in a radio over fiber link, and a significant challenge in link design is finding the right balance between cost and performance for this component.

1.3 Basic Radio Signal Generation and Transportation Methods

In this section, a brief overview of how to generate and transport radio signal over an optical fiber in RoF networks is given. Virtually all of the optical links transmitting microwave/mm-wave signals apply intensity modulation of light [16]. Essentially, three different methods exist for the transmission of microwave/mm-wave signals over optical links with intensity modulation:

- (1) direct intensity modulation,
- (2) external modulation, and
- (3) remote heterodyning.

In direct intensity modulation an electrical parameter of the light source is modulated by the information-bearing RF signal. In practical links, this is the current of the laser diode, serving as the optical transmitter. The second method applies an unmodulated light source and an external light intensity modulator. This technique is called *external modulation*. In a third method, RF signals are optically generated via *remote heterodyning*, that is, a method in which more than one optical signal is generated by the light source, one of which is modulated by the information-bearing signal and these are mixed or heterodyned by the photodetector or by an external mixer to form the output RF signal.

Direct intensity modulation is the simplest of the three solutions. So it is used everywhere that it can be used. When it is combined with direct detection using PD, it is frequently referred to as intensity-modulation direct-detection (IMDD) (Fig.1.1). A direct-modulation link is so named because a semiconductor laser directly converts a small-signal modulation (around a bias point set by a dc current) into a corresponding small-signal modulation of the intensity of photons emitted (around the average intensity at the bias point). Thus, a single device serves as both the optical source and the RF/optical modulator (Fig.1.1). One limiting phenomenon to its use is the modulation bandwidth of the laser. Relatively simple lasers can be modulated to frequencies of several gigahertz,

say, 5.10 GHz. Although there are reports of direct intensity modulation lasers operating at up to 40 GHz or even higher, these diodes are rather expensive or nonexistent in commercial form. That is why at higher frequencies, say, above 10 GHz, external modulation rather than direct modulation is applied. In entering into the millimeter band a new adverse effect, such as the nonconvenient transfer function of the transmission medium, is observed. It turns out that the fiber dispersion and coherent mixing of the sidebands of modulated light may cause transmission zeros, even in the case of rather moderate lengths of fiber. For example, a standard fiber having a one km length has a transmission zero at 60 GHz if 1.55 μm wavelength light is intensity modulated. Due to this phenomenon, optical generation rather than transmission of the RF signal is preferable.

Because the number of BSs is high in RoF networks, simple and cost-effective components must be utilized. Therefore, in the uplink of an RoF network system, it is convenient to use direct intensity modulation with cheap lasers; this may require downconversion of the uplink RF signal received at the BS. In the downlink either lasers or external modulators can be used.

1.4 RoF Link Configuration

In this section we discuss a typical RoF link configuration, which is classified based on the kinds of frequency bands (baseband (BB), IF, RF bands) transmitted over an optical fiber link. Representative RoF link configurations are schematically shown in Fig. 1.2[16]. Here, we assume that a BS has its own light source for explanation purpose. In each configuration of the figure, BSs do not have any equipment for modulation and demodulation, only the CS has such equipment.

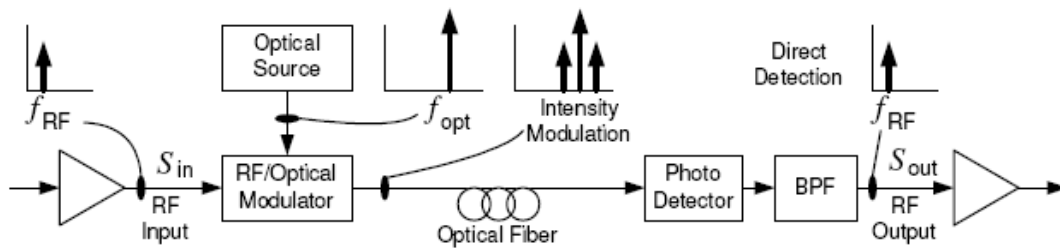


Figure 1.1. IMDD Analog optical link

In the downlink from the CS to the BSs, the information signal from a public switched telephone network (PSTN), the Internet, or other CS is fed into the modem in the CS. The signal that is either RF, IF or BB bands modulates optical signal from LD. As described earlier, if the RF band is low, we can modulate the LD signal by the signal of the RF band directly. If the RF band is high, such as the mm-wave band, we sometimes need to use external optical modulators (EOMs), like electroabsorption ones. The modulated optical signal is transmitted to the BSs via optical fiber. At the BSs, the RF/IF/BB band signal is recovered to detect the modulated optical signal by using a PD. The recovered signal, which needs to be upconverted to RF band if IF or BB signal is transmitted, is transmitted to the MHs via the antennas of the BSs.

In the configuration shown in Fig. 1.2, the modulated signal is generated at the CS in an RF band and directly transmitted to the BSs by an EOM, which is called *RF-over-Fiber*. At each BS, the modulated signal is recovered by detecting the modulated optical signal with a PD and directly transmitted to the MHs. Signal distribution as RF-over-Fiber has the advantage of a simplified BS design but is susceptible to fiber chromatic dispersion that severely limits the transmission distance [15-15].

In the configuration shown in Fig. 1.2 (b), the modulated signal is generated at the CS in an IF band and transmitted to the BSs by an EOM, which is called *IF-over-Fiber*. At each BS, the modulated signal is recovered by detecting the modulated optical signal with a PD, upconverted to an RF band, and transmitted to the MHs. In this scheme, the effect of fiber chromatic dispersion on the distribution of IF signals is much reduced, although antenna BSs implemented for RoF system incorporating IF-over-Fiber transport require additional electronic hardware such as a mm-wave frequency LO for frequency up- and

downconversion. In the configuration (c) of the figure, the modulated signal is generated at the CS in baseband and transmitted to the BSs by an EOM, which is referred to as *BB-over-Fiber*. At each BS, the modulated signal is recovered by detecting the modulated optical signal with a PD, upconverted to an RF band through an IF band or directly, and transmitted to the MHs. In the baseband transmission, influence of the fiber dispersion effect is negligible, but the BS configuration is the most complex. Since, without a subcarrier frequency, it has no choice but to adopt time-division or code-division multiplexing. In the configuration shown in Fig. 1.2 (d), the modulated signal is generated at the CS in a baseband or an IF band and transmitted to the BSs by modulating a LD directly. At each BS, the modulated signal is recovered by detecting the modulated optical signal with a PD, upconverted to an RF band, and transmitted to the MHs. This is feasible for relatively low frequencies, say, less than 10 GHz.

By reducing the frequency band used to generate the modulated signal at the CS such as *IF-over-Fiber* or *BB-over-Fiber*, the bandwidth required for optical modulation can greatly be reduced. This is especially important when RoF at mm-wave bands is combined with dense wavelength division multiplexing (DWDM) as will be discussed in section 3.3.5. However, this increases the amount of equipment at the BSs because an upconverter for the downlink and a downconverter for the uplink are required. In the RF subcarrier transmission, the BS configuration can be simplified only if a mm-wave optical external modulator and a high-frequency PD are respectively applied to the electric-to-optic (E/O) and the optic-to-electric (O/E) converters.

For the uplink from an MH to the CS, the reverse process is performed. In the configuration shown in Fig. 1.2 (a), the signals received at a BS are amplified and directly transmitted to the CS by modulating an optical signal from a LD by using an EOM. In the configuration (b) and (c), the signals received at a BS are amplified and downconverted to an IF or a baseband frequency and transmitted to the CS by modulating an optical signal from a LD by using an EOM. In the configuration (d), the signals received at a BS are amplified and downconverted to an IF or a baseband frequency and transmitted to the CS by directly modulating an optical signal from a LD.

1.5 1.5 State-of-the-Art Millimeter-wave Generation and Transport Technologies

Recently, a lot of research has been carried out to develop mm-wave generation and transport techniques, which include the optical generation of low phase noise wireless signals and their transport overcoming the chromatic dispersion in fiber. Several state-of-the-art techniques that have been investigated so far are described in this section, which are classified into the following four categories [17]:

1. optical heterodyning[18]
2. external modulation [19]
3. up- and down-conversion [20]
4. optical transceiver [21]

1.6 Optical Heterodyning

In optical heterodyning technique, two or more optical signals are simultaneously transmitted and are heterodyned in the receiver. One or more of the heterodyning products is the required RF signal. For example, two optical signals with a wavelength separation of 0.5 nm at 1550 nm will generate a beat frequency of around 60 GHz. Heterodyning can be realized by the PD itself or the optical signals can be detected separately and then converted in an electrical (RF) mixer. In a complete (duplex) system, the PD can be replaced by an electroabsorption transceiver.

Because phase noise is a key problem in digital microwave/mm-wave transmission, care must be taken to produce a small phase noise only by the heterodyned signals. This can be achieved if the two (or more) optical signals are phase coherent; in turn, this can be realized if the different frequency optical signals are somehow deduced from a common source or they are phase-locked to one master source. Benefits of this approach are that (1) it overcomes chromatic dispersion effect and (2) it offers a flexibility in frequency since frequencies from some megahertz up to the terahertz-region is possible. However, it uses either a precisely biased electrooptic modulator or sophisticated lasers[22]

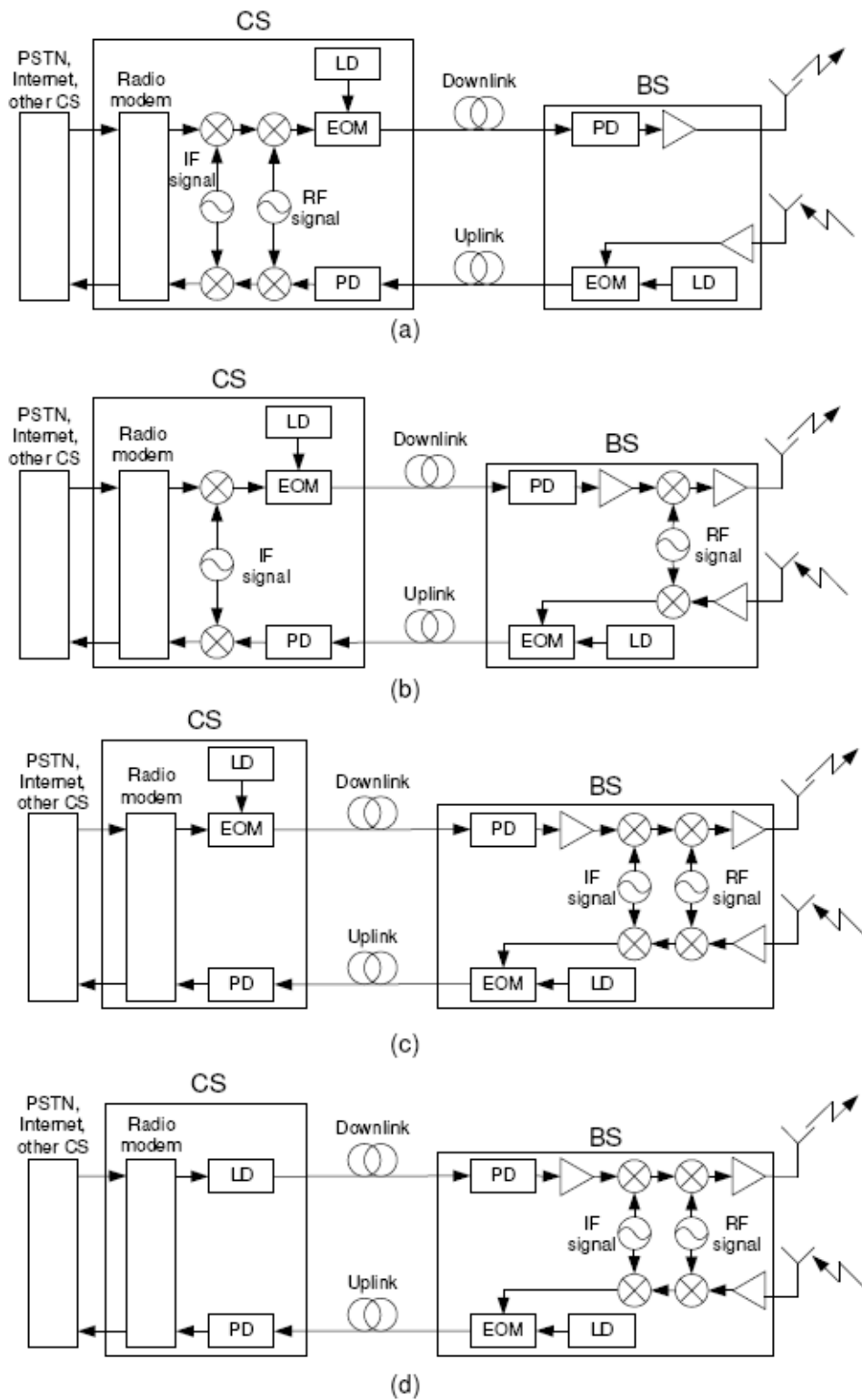


Figure 1.2: Representative RoF link configurations. (a) EOM, RF modulated signal. (b) EOM, IF modulated signal, (c) EOM, baseband modulated signal. (d) Direct modulation.

Fig. 1.3 shows a typical design of optical heterodyning. The master laser's intensity is modulated by the unmodulated RF reference signal; several harmonics of the reference signal and consequently several sidebands are generated. The reference laser is injection locked by one of these and the signal laser by another one in such a way that the difference of their frequencies corresponds to the mm-wave local oscillator frequency. And, as seen, the optical field generated by the signal laser is also modulated by the information-bearing IF signal.

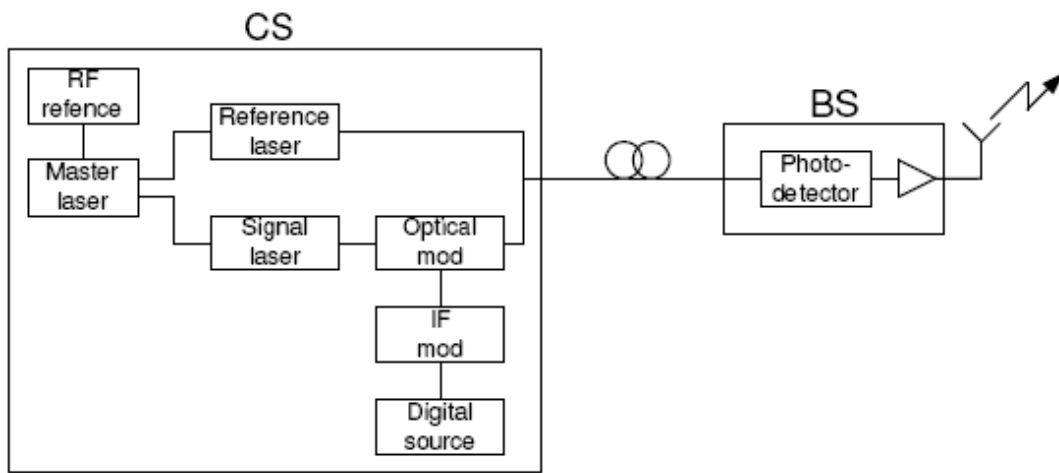


Figure 1.3: Optical heterodyning

1.7 Optical Transceiver

The simplest BS structure can be implemented with an optical transceiver such as electro-absorption transceiver (EAT). It serves both as an O/E converter for the downlink and an E/O converter for the uplink at the same time. Two wavelengths are transmitted over an optical fiber from the CS to BS. One of them for downlink transmission is modulated by user data while the other for uplink transmission is unmodulated. The unmodulated wavelength is modulated by uplink data at the BS and returns to the CS. That is, an EAT

is used as the photodiode for the data path and also as a modulator to provide a return path for the data, thereby removing the need for a laser at the remote site. This device has been shown to be capable of full duplex operation in several experiments at mm-wave bands[31] . A drawback is that it suffers from chromatic dispersion problem. Fig. 1.4 shows an RoF system based on EAT. Note that two wavelengths are always needed for up- and downlink communication, and full-duplex operation is possible.

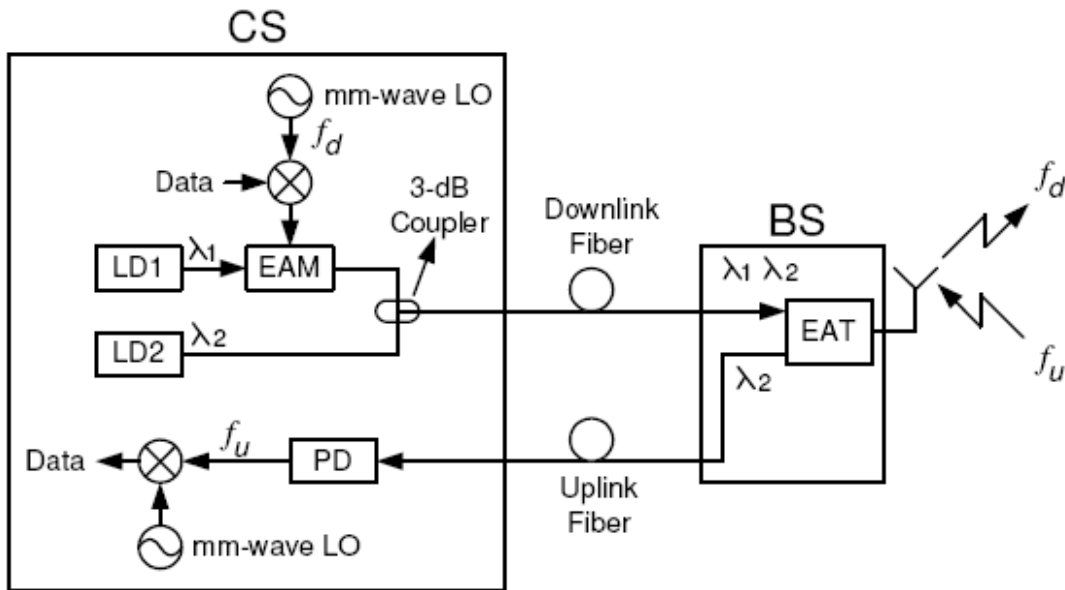


Figure 1.4 : Electroabsorption transceiver (EAT).

1.8 RoF and Wavelength Division Multiplexing (WDM)

The application of WDM in RoF networks has many advantages including simplification of the network topology by allocating different wavelengths to individual BSs, enabling easier network and service upgrades and providing simpler network management. Thus, WDM in combination with optical mmwave transport has been widely studied. A schematic arrangement is illustrated in Fig. where for simplicity, only downlink transmission is depicted. Optical mm-wave signals from multiple sources are multiplexed

and the composite signal is optically amplified, transported over a single fiber, and demultiplexed to address each BS. Furthermore, there have been several reports on dense WDM (DWDM) applied to RoF networks. Though a large number of wavelengths is available in the modern DWDM technologies, since mm-wave bands RoF networks may require even more BSs wavelength resources should be efficiently utilized.

A challenging issue is that the optical spectral width of a single optical mm-wave source may approach or exceed WDM channel spacing. For example, Fig. 1.6 shows an optical spectrum of DWDM mm-wave RoF signals with optical DSB modulation (a) and SSB modulation (b), where we assume that the carrier frequency of the mm-wave signal is 60 GHz. Fig. 1.6 (a) indicates that to transmit single data channel at 60 GHz band, more than 120 GHz bandwidth is necessary for DSB modulation. In addition, from a viewpoint of cost reduction, it is preferable to use the channel allocation in accordance with ITU grid because of the availability of optical components. Then, the minimum channel spacing in this case is 200 GHz. In case of SSB modulation, this is 100 GHz as shown in Fig.1.6 (b). To increase the spectral efficiency of the system, the concept of optical frequency interleaving has been applied.

Another issue is related to the number of wavelengths required per BS. It is desirable to use one wavelength to support full-duplex operation. In [1], a wavelength reuse technique has been proposed, which is based on recovering the optical carrier used in downstream signal transmission and reusing the same wavelength for upstream signal transmission.

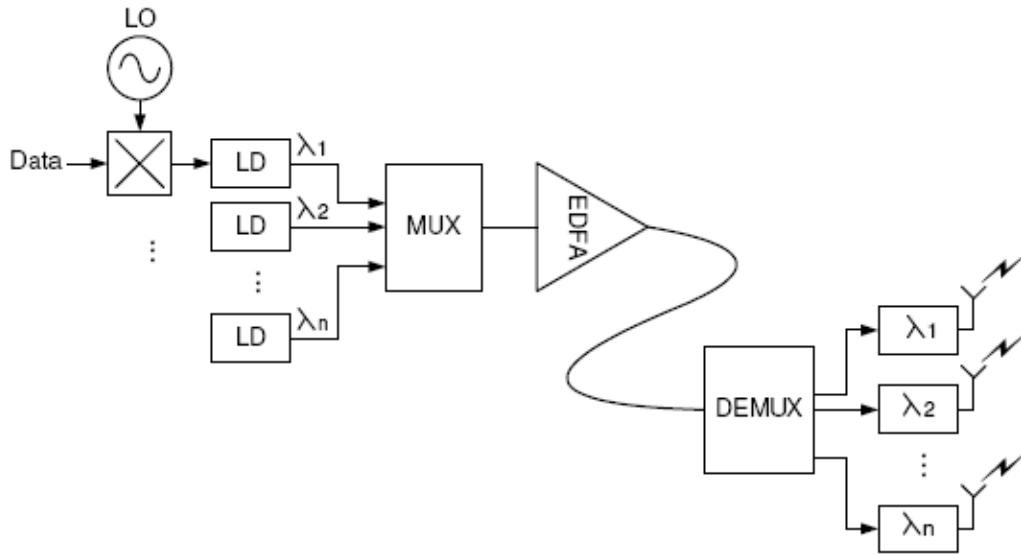


Figure 1.5: Schematic illustration of a combination of DWDM and RoF transmission.

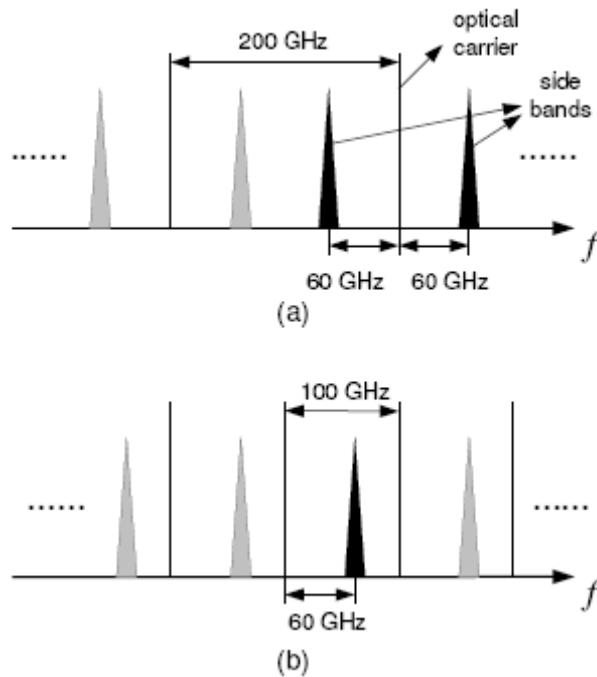


Figure 1.6: Optical spectra of DWDM mm-wave RoF signals of conventional optical (a) DSB and (b) SSB.

Fig. 1.7 shows a typical unidirectional fiber ring architecture that can be used for the delivery of broadband wireless services . In the CS, all down- and uplink light sources are multiplexed and amplified. The modulated downlink channels and the unmodulated uplink channels are fed into the fiber backbone of the ring network. At each BS, a pair of down- and uplink wavelengths is dropped through an OADM to the EAT, which simultaneously detects and modulates the down- and uplink channel, respectively. The modulated uplink channels are added to the backbone again, looped back to the CS, where they are demultiplexed and detected. The major advantage of this point-to-multipoint WDM ring network is the centralization of all required light sources in the CS, allowing for a simple BS configuration.

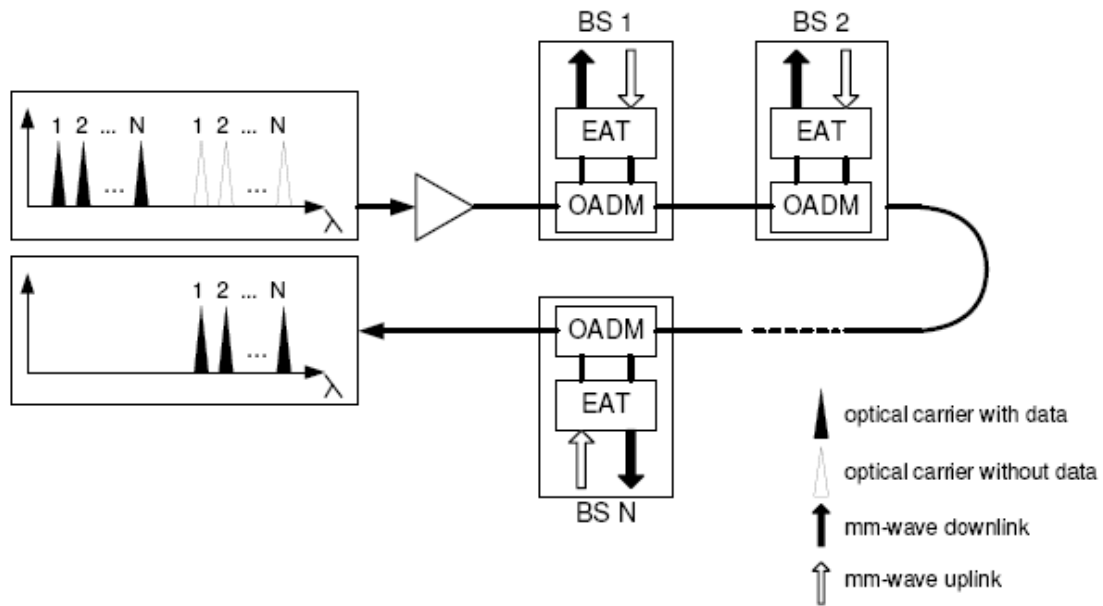


Figure 1.7: RoF ring architecture based on DWDM

1.9. Basic Microwave Characteristics of RoF Links

1.9.1 Insertion Loss

Loss is proportional to the square of the optical loss (reason: in the photodetector photons generate electrons; i.e: electrical current is proportional to optical power). Under appropriate matching conditions loss can be very low, even an insertion gain is possible in this seemingly passive system.

1.9.2 Noise Figure F

Noise figure is an important microwave parameter, defined as the ratio of the input SNR to the output SNR of the link. While L is minimal in the case of matched impedances, minimal F requires different generator and load impedances. In contrast to purely electrical transducers, F can be lower than L e.g. in a practical example

$$F_{dB} = L_{dB} / 2 + 6.8$$

1.9.3 Optical Impairments

Optical impairments such as fiber chromatic dispersion and fiber nonlinearity have increased microwave effects. For microwave frequencies, these effects become even more pronounced. Thus proper compensation of these effects is to be done for better transmission characteristics.

1.9.4. Bandwidth

The achievable bandwidth of the RoF is limited by the RoF components. Also the laser diode and the photo detector impedances are also factors that pose grave issues to the achievable bandwidth. In an optical microwave link operating at 10 GHz microwave frequency and carrying a 156 Mbps QPSK signal, the useful bandwidths about 10GHz±40MHz are obtainable.

1.9.5. Dynamic Range

The Dynamic range of the RoF link is defined as The ratio of the maximum achievable signal to noise ratio to the minimum Signal to noise ratio needed for the link. The

maximum SNR is dependent on the maximum transmitted power which in turn is limited by the laser saturation. Therefore the bias current should be chosen carefully as the link performance depends upon it.

Another factor that limits The DR is the Relative intensity noise (RIN) from the laser. The RIN depends on the bias current approximately as the square of the bias current. As the bias current increases, the RIN also increases thus reducing the DR. Thus we see that the effect of the bias current on the DR is twofold.

1.10. RoF ARCHITECTURE FOR CELLULAR WIRELESS NETWORKS

In a network in which transfer is realized via RoF the physical layer is essentially composed of two sub-layers: conventional wireless layer and below it the optical layer. In the solution being simplest from the conceptual point of view the optical layer forms a star network: point-to-point RoF links join the base stations to a central station – one fiber to one BS. However, more sophisticated solutions are desirable, as in the present application number of the base stations is rather high. If a fiber serves more than one base station, the optical layer implements a second multiple access (MA) system, independent from the conventional, wireless MA. In Fig 1.2 conceptual drawing of this double MA system is shown. In this architecture a fiber backbone is laid and each base station is connected to it resulting in an bus network. And an suitable MA technique is applied to provide access to each base station. MA techniques applied in the optical layer can be very diverse: sub-carrier multiplexing (SCM), TDMA, CDMA, WDM (wavelength division multiplexing).

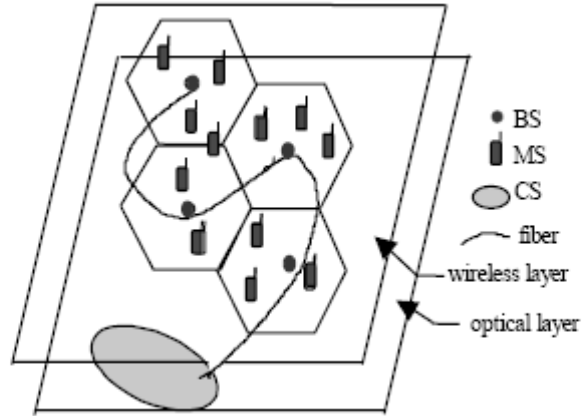


Figure 1.8. Conceptual drawing of a double-MA wireless network

However as optical technology of wavelength division is well-evolved one fiber can serve very different services simultaneously: signals of different services can be transmitted via different wavelengths. Different services can operate with different radio frequencies, different RF modulation, with different cellular structure etc. Services can be mobile, fixed wireless access, narrow band or wide band or whatever. Thus RoF can be regarded and applied as a transfer network of universal use. In multiservice RoF each service operates with different optical wavelength; at BS and CS, signal of the relevant wavelength is only accessible (separated via appropriate optical multiplexers).

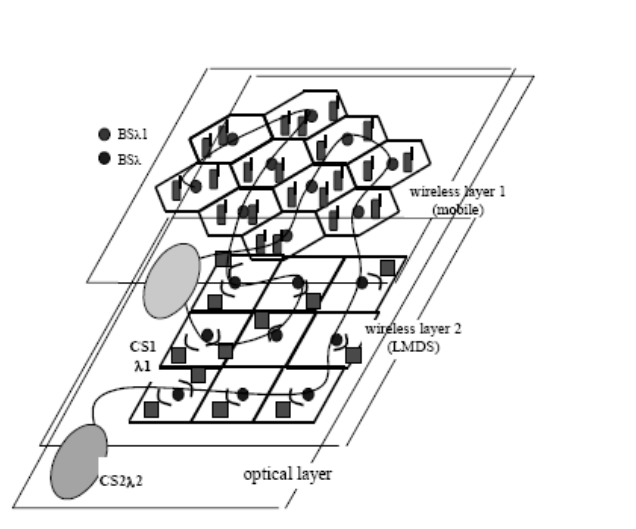


Figure 1.9. A two-service WDM optical transfer network

1.11. ADVANTAGES OF RoF

The use of RoF in Mobile Communication Networks is

- Low RF power remote antenna units(RAUs);
- Line of Sight operation (multipath effects are minimized);
- Enabling of mobile broadband radio access close to the user in an economically accepted way.
- Reduced environmental impact due to small RAUs.
- Good coverage.
- Capacity enhancement by means of improved trunking efficiently;
- Dynamic radio resource configuration and capacity allocation;
- Alleviation of the cell planning problem;
- Reduction in the number of handovers;
- Centralized upgrading or adaptation;
- High reliability and low maintenance costs.
- Support for future broadband multimedia applications;
- Better coverage and increased capacity;
- High quality signals;
- Support for macrodiversity transmission;
- Low fiber attenuation;
- Reduced engineering and system design costs;
- Multiple services on a single fiber;
- Lightweight fiber cables;
- No electromagnetic interference;
- High reliability.

The use of low power RAUs has following benefits

- Low generated interference;
- Increased efficiency;
- Easier frequency/network planning;

- Increased battery lifetime of mobile terminals;
- Relaxed human health issues;
- The potential to use RF CMOS technology in the mobile terminals.

2. APPLICATIONS OF ROF:

2.1 Introduction

Since the RoF networks are going to be the backbone of the future communication systems, a glimpse into their possible applications and advantages they offer over the existing technologies need to be dealt with. In this chapter various applications of the RoF are discussed in detail. These applications are mainly intended to use the RoF technology for the next generation wireless access systems.

2.2 Fiber to the Home/Fiber to the Premises(FTTH/FTTP)

The conventional access network infrastructures, namely the twisted-pair telephony networks and the coaxial cable CATV networks, are having a hard time to keep up with these traffic demands. Digital subscriber line

Techniques (ADSL, VDSL, etc.) and cable modem techniques are evolving into higher speeds, but at the cost of a shorter reach. The unique properties of optical single-mode fiber being its low loss and extremely wide inherent bandwidth make it the ideal candidate to meet the capacity challenges for now and the foreseeable future. The costs of digging and ducting are the major cost items in access networks, outweighing by far the costs of the transmission medium and the line terminating equipment. Civil works typically may take some 85% of fiber to the home (FTTH) first installed network costs, while the fiber cable and the optical components take only 3%; the remainder is taken by

other hardware, installation activities, and other services. Hence, in green-field situations, the costs of introducing FTTH may not differ much from, e.g., twisted copper pair or coaxial cable access solutions. Moreover, the costs of fiber-optic line-terminating transceivers are coming down rapidly. FTTH's operational costs may be lower, as it needs less active equipment in the field which needs maintenance.

A fiber link can basically handle any kind of access traffic, so installing fiber is an insurance for the future (B future-proof, or B forecast-tolerant, investment).

2.2.1 Fiber Access network Architectures

Basically, three architectures may be deployed for the fiber access network .

1. **Point-to-point architecture**, where individual fibers run from the local exchange to each home. Many fibers are needed, which entails high first installation costs, but also provides the ultimate capacity and the most flexibility to upgrade services for customers individually. In the local exchange, as many fiber terminals are needed as there are homes, so floor space and powering may become issues.

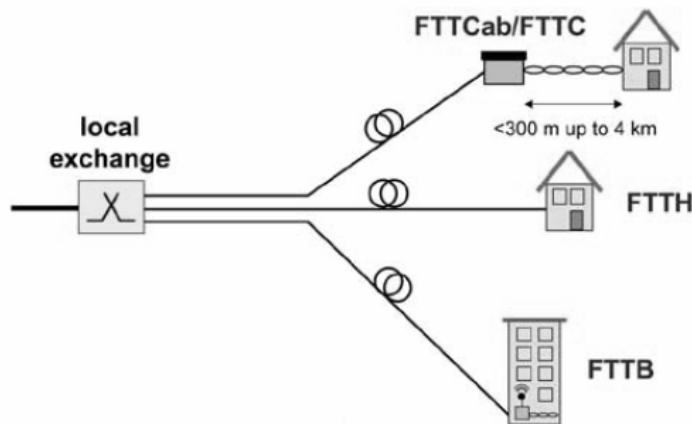


Figure 2.1. Point to point architecture.

2. **Active star architecture**, where a single fiber carries all traffic to an active node close to the end users, from where individual fibers run to each cabinet/home/building. Only a single feeder fiber is needed, and a number of short branching fibers to the end users, which reduces costs; but the active node needs powering and maintenance. It also needs to withstand a wider range of temperatures than in-door equipment. In network upgrade scenarios, from the active node twisted copper pair lines (such as for ADSL up to some 4 km at speeds up to some 6 Mbit/s, or VDSL at speeds up to some 50 Mbit/s for lengths of some 500 m) may run, or coaxial cable lines (such as for HFC), or even wireless links to the customer [fixed wireless access (FWA)]. The active node may be located in a cabinet at the street curb site (fiber to the cabinet (FTTCab) or FTTC), or in the basement of, e.g., a multidwelling units building [fiber to the building (FTTB)] from where the communication traffic is run throughout the building by copper wired and wireless local area networks at 100+ Mbit/s speeds.

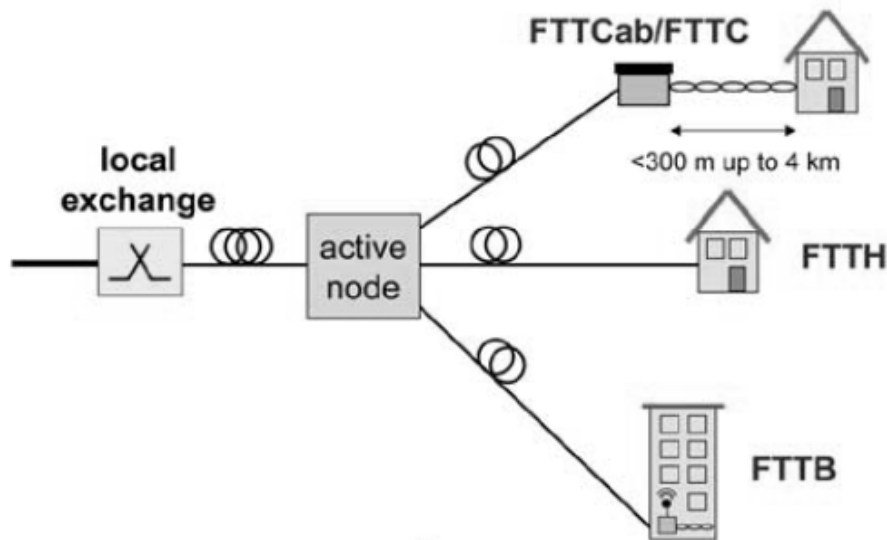


Figure 2.2. Active star architecture

3. **Passive star architecture**, in which the active node of the active star topology is replaced by a passive optical power splitter/combiner that feeds the individual short branching fibers to the end users. In addition to the reduced installation costs

of a single fiber feeder link, the completely passive nature of the outside plant avoids the costs of powering and maintaining active equipment in the field. This topology has therefore become a very popular one for introduction of optical fiber into access networks, and is widely known as the passive optical network (PON).

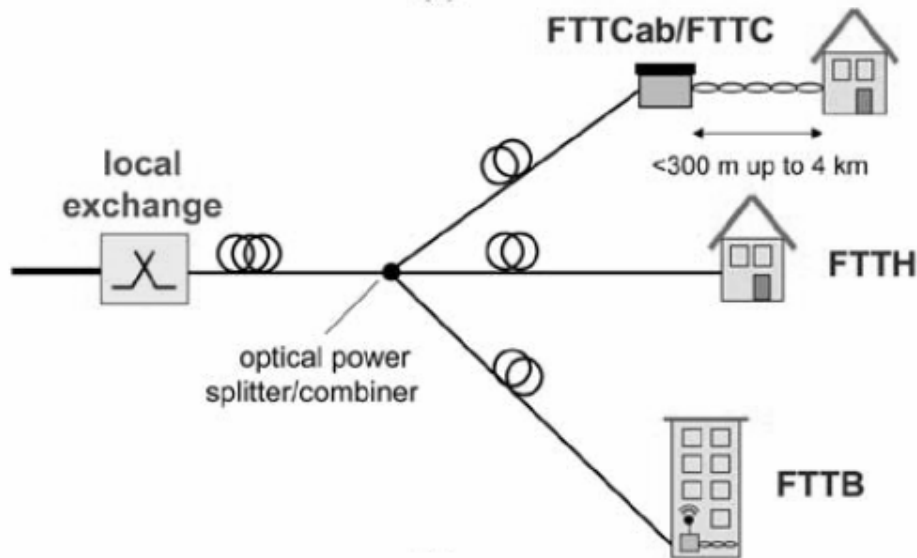


Figure 2.3. Passive Star Architecture.

2.3. Radio-over-Fiber Links for Indoor Wireless LANs:

The demand for broadband services has driven research on millimeter-wave frequency band communications for wireless access networks such as picocellular mobile systems and indoor wireless local area networks (LANs). The millimeter-wave band is considered to be a promising solution owing to its spectrum availability, compact size of radio frequency (RF) devices. Especially, signals at around 60 GHz with severe atmospheric attenuation due to oxygen absorption provide the excellent frequency reusability between adjacent picocell coverage ranges. The mm-wave signals, however, suffer from severe loss along the transmission line as well as atmospheric attenuation. Low-attenuation, EMI-free optical fiber transmission is considered attractive for long-haul transport of millimetric frequency band wireless signals. Among system options for such radio-over-

fiber (ROF) systems, the intermediate frequency (IF) feeder is considered to be the cost-effective, practical and relatively flexible system configuration.

The system consists of OFDM modems, baseband signal processing modules, IF modules that convert baseband signals to 2.5GHz frequency band signals, an optical single mode fiber link, mm-wave transmitter/receiver that converts the IF signals into 60GHz frequency band signals and 60GHz ones into IF ones, respectively, and mm-wave band antennas. Generation and reconstruction algorithms for 16-QAM (quadrature amplitude modulation) OFDM signals are carried out by the OFDM modems. Digital-to-analog (D/A) and analog-to-digital (A/D) converters are remotely controlled, and IF modules correspond to a L-band up-converter from the baseband into the 2.5GHz band and an L-band down-converter .

The optical link contains optical-to-electrical (O/E) and electrical-to-optical (E/O) converters with a distributed feedback laser diode (DFB-LD) as a 2.5GHz optical signal to 2.5GHz frequency band signals, an optical single mode fiber link, mm-wave transmitter/receiver that converts the IF signals into 60GHz frequency band signals and 60GHz ones into IF ones, respectively, and mm-wave band antennas. Generation and reconstruction algorithms for 16-QAM (Quadrature amplitude modulation) OFDM signals are carried out by the OFDM modems. Digital-to-analog (D/A) and analog-to-digital (A/D) converters are remotely controlled, and IF modules correspond to a L-band up-converter from the baseband into the 2.5GHz band and an L-band down-converter with reverse band shifting.

The optical link contains optical-to-electrical (O/E) and electrical-to-optical (E/O) converters with a distributed feedback laser diode (DFB-LD) as a 2.5GHz optical signal generator with direct modulation. The 2.5GHz IF signals are mixed in the mm-wave transmitter with 57.2GHz signals from the local oscillator (LO) and are converted to OFDM signals with a center frequency of 59.7GHz. They are then transported to a power amplifier and an antenna. The reverse order action is performed in the mm-wave receiver. At an IF down converter, the resulting IF OFDM signal is converted to the base band signal to be sampled by an analog-to-digital converter (ADC). The sampled sequence of the received OFDM signal is processed to recover the original data. generator with direct modulation. The 2.5GHz IF signals are mixed in the mm-wave transmitter with 57.2GHz

lack of available vacant frequency band, the frequency band of 4G systems is expected to be higher than 3.0 GHz. In case of WiBro, its frequency band is 2.3 GHz which is higher than 3G frequency. This increased frequency band leads to the high radio-wave propagation loss for uplink and downlink, as shown in following figure. In particular, the high propagation loss for uplink increases the power consumption of the mobile handsets. Network operators for 4G will be having tremendous difficulties accommodating the increasing traffic, because the system should guarantee the high data rate for each user.

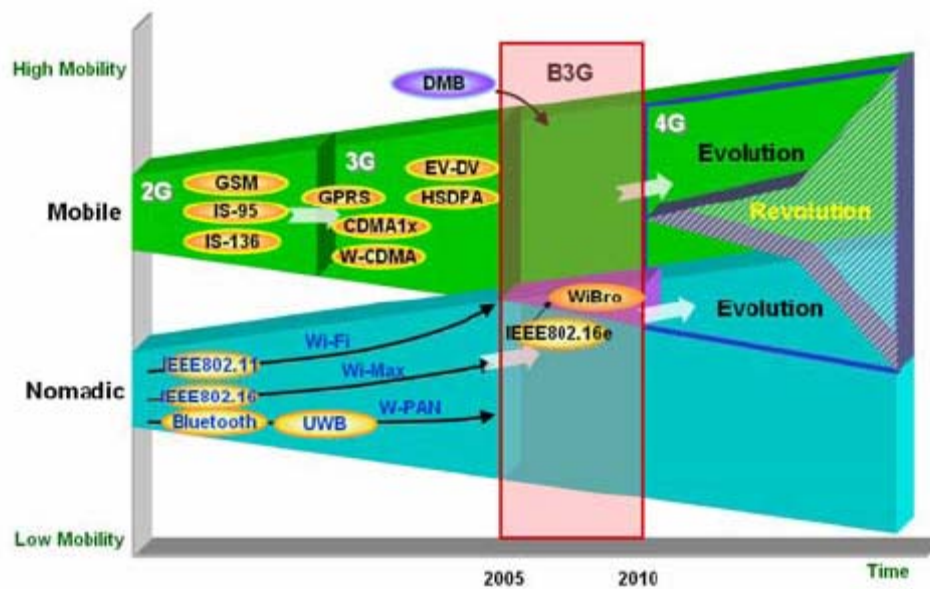


Figure 2.5. Evolution of various wireless networks

RoF technology is one of the best solutions for the implementation of the reduced cell size and the centralization of base station . Using optical fiber with ultra-wide bandwidth, it is possible to transfer the complicated RF modem and signal processing functions to a centralized control station, so called base station hotel. It enables us to implement compact and cost effective remote access units. In addition, RoF links can support a variety of wireless systems, regardless of their frequency bands, because they have ultra-wide bandwidth and protocol transparent characteristics.

Nowadays, customers expect their mobile terminals to work whether inside or outside the building. Particularly, in-building environment has many difficulties in providing various

wireless services because it has a large propagation loss due to a myriad of obstacles. RoF technology can transmit a variety of wireless services over a strand of fiber and make small size remote access units. Moreover, it is suitable for present and future wireless services such as 4G. Therefore, we are developing RoF technologies providing multiple wireless systems including 3G, WLAN, Digital multimedia broadcasting (DMB), and B3G at the hot spot or in-building area.

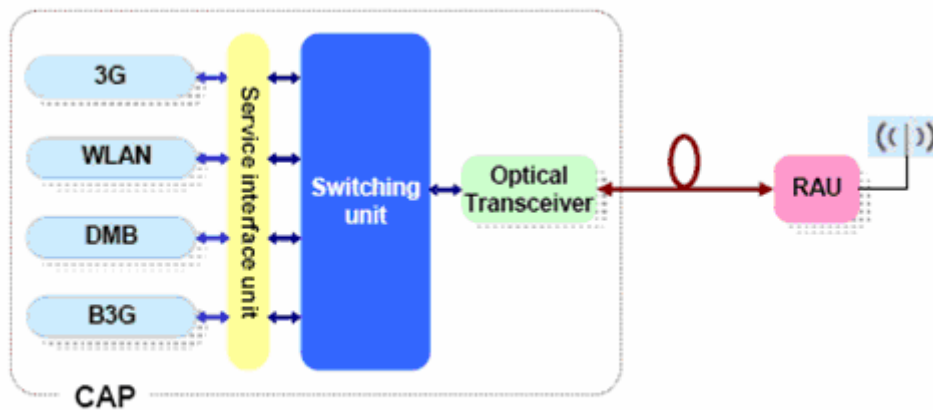


Figure 2.6. RoF for 3G and 4G.

2.5. Radio-over-Fiber Network for Microcellular System:

In this architecture, the traditional macrocell is divided into microcells. At BS, the output of a Nd:YAG laser is split by a $1 \times N_1 N_R$ star coupler and externally modulated by a group of $N_1 N_R M$ SCM RF signals through a Mach-Zehnder Modulator. Each group contains M subcarriers. In fact N_1 groups of RF subcarriers are reused N_R times in the whole macrocell, so the total channel number provided by this single laser is $N_1 N_R M$. In following figure microcells 1A, 1B and 1C use the same frequency. Such idea is exactly same as that used in the current mobile phone system so that no additional effort is needed for the frequency planning except that the cochannel interference may have to be considered due to the different power levels in the microcellular system.

At RP's, as shown in Fig. 2, downlink signals are detected by one photodetector with a low-noise amplifier (LNA) and then amplified by a power amplifier before transmitting through the antenna. An optical coupler with the coupling ratio $C_D:C_U$, where $C_D+C_U=1$, is placed at the input of the RP to reserve some portion of the optical power for uplink transmission. The reserved optical power is remodulated by radio signals received from the antenna through an AM modulator and detected at BS with a separate PIN photo detector for each uplink. This distribution structure has the following **advantages over** those using two distributed feedback (DFB) lasers and direct modulation scheme at both BS's and RP's

1. **High-power Nd:YAG lasers**, suitable for a high-fanout distribution system, are available, and their relative intensity noise (RIN) can be as low as 165 dB/Hz.
- 2 **Reduced power consumption** and complexity of RP's due to the use of external modulators.
- 3 **Excellent performance of AM modulation** and its associated low IMD's, which will increase the system dynamic range (DR) significantly.

Although the external modulator is sensitive to the polarization state of the input optical beam, one polarization controller located in front of the $1 \times N_I N_R$ coupler is enough to maintain the input beam of AM modulators at the BS at the desired polarization state. For RP's, the automatic polarization controller can be used. Another solution is to remove this polarization controller to the output of the modulator at the BS and let it be controlled by the detected signal level at the BS receiver. It can reduce the complexity of RP's.

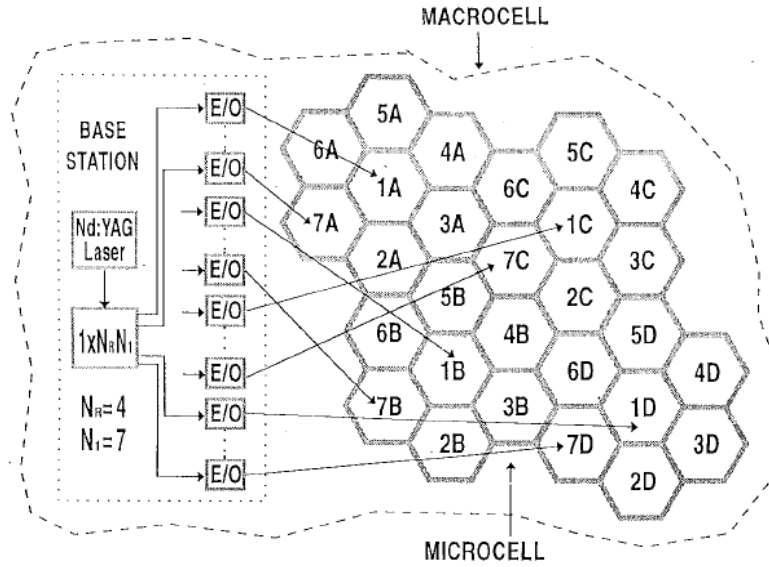


Figure 2.7. Conceptual diagram for the RoF distribution system with the frequency reuse

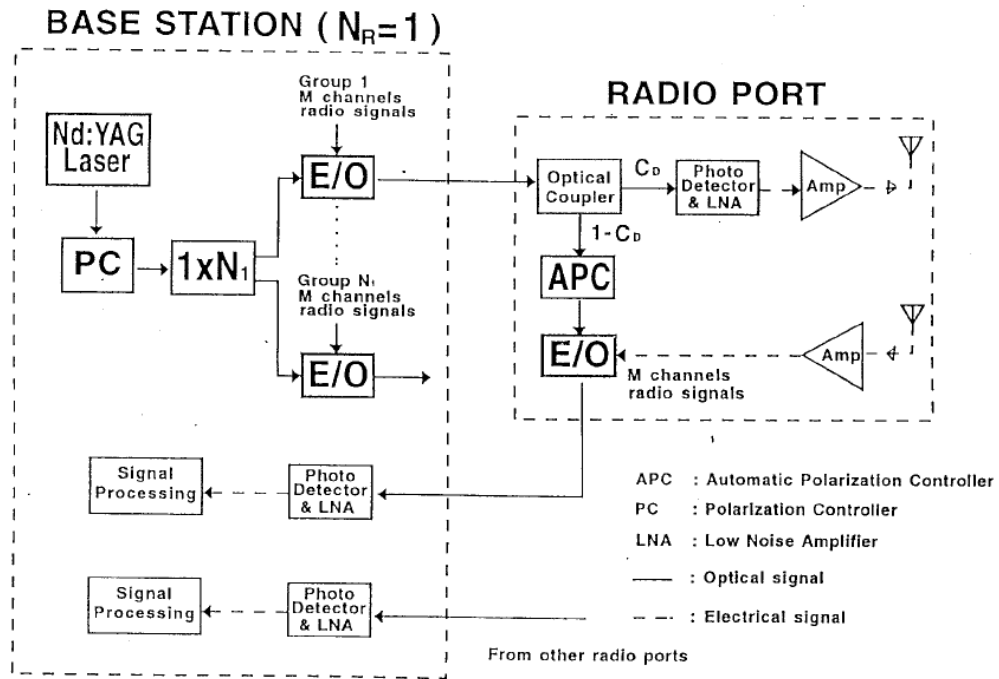


Figure 2.8 Block diagram of the fiber-radio link.

2.6. RoF Network Architecture for Road Vehicle Communication Systems:

The demand for intelligent transportation systems (ITSs) using the latest mobile communication technologies continues to increase to exchange traffic information and achieve safe, smooth, and comfortable driving. These systems can be categorized into road vehicle communication (RVC) systems and inter-vehicle communication (IVC) systems. The RVC system is an infrastructure network for ITS which will be deployed along the road.

One *promising alternative* to the first issue is a radio over fiber (ROF) fed network since in this network functionally simple and cost-effective BSs (in contrast to conventional wireless systems) are utilized. In particular, a large number of BSs, which are deployed along the road and serve as remote antenna units for MHS, are interconnected with a control station (CS) that performs all processing such as modulation/demodulation, routing, medium access control (MAC) and so on. This configuration leads to a centralized network architecture that could efficiently be used for resource management.

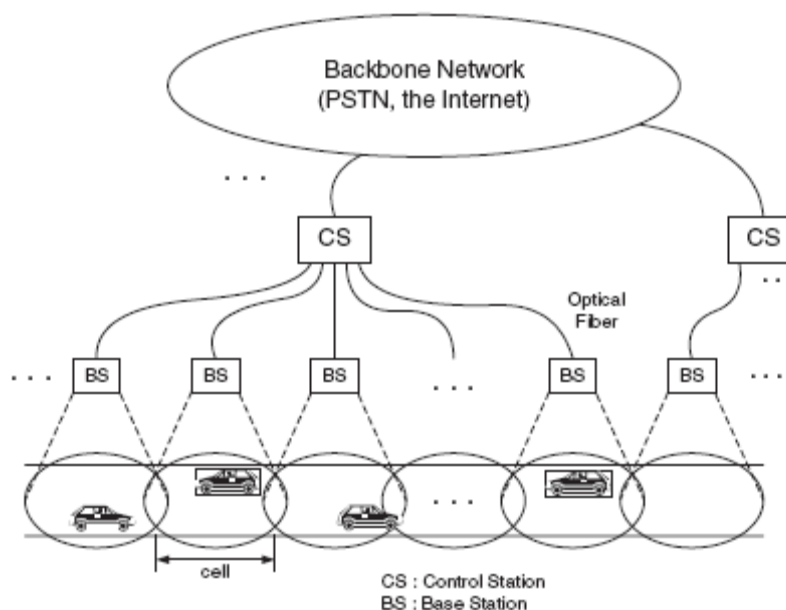


Figure 2.9. A vehicle communication system

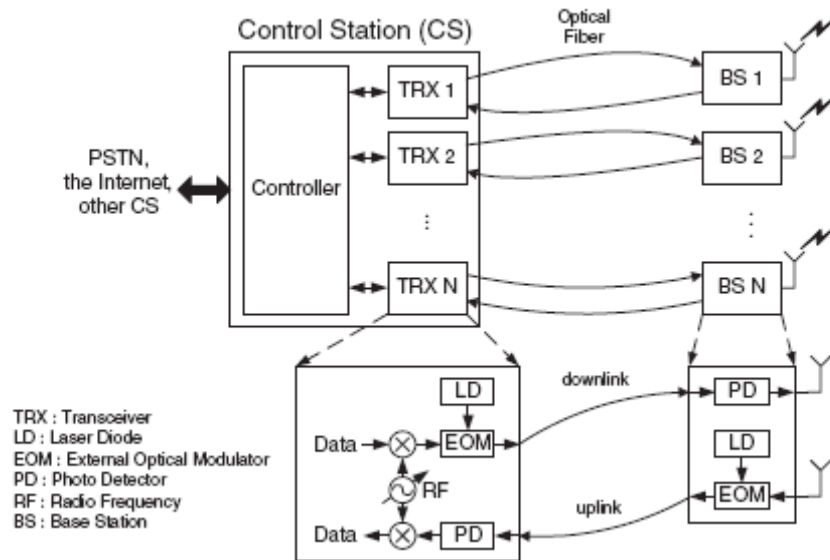


Figure 2.10 Architecture of the control station and the base station.

2.7. RADIO OVER FIBER FOR IN BUILDING MOBILE COMMUNICATIONS:

In-building coverage is an important and growing market for cellular network operators, who wish to gain and retain customers in environments such as corporate office buildings, shopping malls and airports. The most effective and efficient way of providing this coverage with good service quality is to place one or more base stations at a central location inside the building and use a distributed antenna system (DAS) transmission infrastructure to distribute the wireless signals from the base stations to the various antenna locations around the building. Although DASs can be constructed using coaxial cable, the preferred option for larger installations is optical fiber cable. This is due to the very high attenuation of coaxial cable, which makes longer transmission spans impractical. Analog optical links using radio over fiber are in use today in many DAS installations around the world.

2.8. Switched RoF Distributed Antenna System (DAS)

As discussed earlier, radio over fiber links are used to construct distributed antenna systems for large inbuilding wireless deployments. A typical DAS is shown in figure.

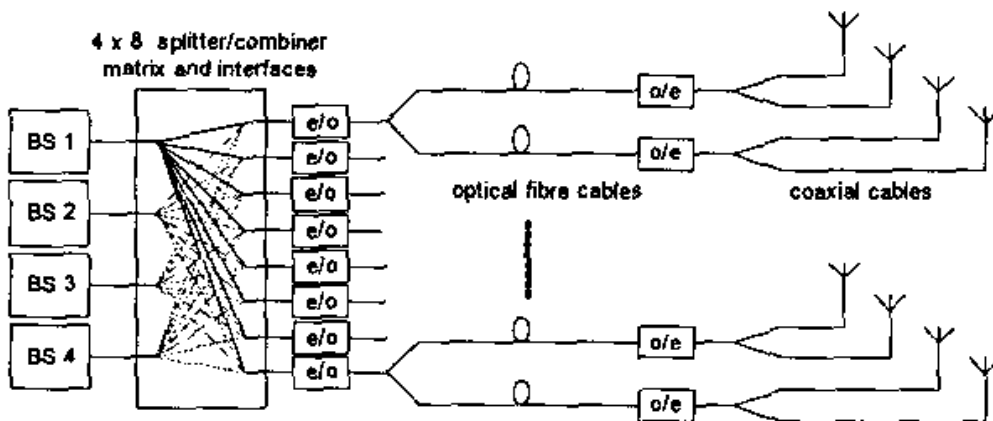


Figure 2.11 Architecture of a Typical Fiber DAS

there are 4 base station inputs, which may be from different operators or offer different services. The base station signals are combined and split to each of the 8 optical drivers (denoted by e/o in the figure) using passive splitter / combiner matrices. The outputs of the 8 lasers are optically split 2 ways and optical fiber cables take the signals to 16 remote antenna units. At each remote antenna unit the optical signals are converted back to the RF domain by the o/e converters (photodiodes), where they are amplified, filtered and split between two antenna connectors. The links between the remote antenna units and the antennas are via short lengths of coaxial cable. This configuration can therefore support an installation with 32 antennas. Each antenna radiates the signals from all 4 base stations, although in some cases an RF patch panel and custom splitters and combiners may be used in place of the splitter / combiner matrices in order to provide different signals to different antenna subsets. This is difficult to arrange in practical situations, especially where the configuration may need to be changed at a later date.

This means that all services and all operators connected to the DAS have the same RF footprint and radio plan. The fixed configuration of a fiber DAS becomes a *significant limitation*, particularly in large buildings and where multiple services or multiple operators share the same DAS. A new DAS architecture, switched-DAS, described here overcome these problems by incorporating a switch matrix in between the base stations and the optical drivers, in place of the fixed splitter / combiner matrices. The DAS itself remains unchanged. The switch matrix enables the operator to dynamically alter the mapping of capacity and services within the network to meet usage demands. Because the switch matrix is under software control, the operator is able to implement any network configuration changes remotely. In many cases, this removes the need for an engineer to visit for service changes.

Typical operational functions enabled by the switch matrix include:

1. Provisioning of services- Services can be simply provisioned over the coverage area by configuring which antennas are connected to each base station. Thus a new service configuration can be deployed remotely and immediately without the need for any site

works.

2. Time of day provisioning- Since the switch matrix configuration can be modified dynamically, it can be modified on a time-of day or day-of-week basis, for example to allow for capacity peaks in areas during commuting rush hour, or to switch capacity to a sporting venue when a match is being played.

3. Capacity management- The capacity requirements of a wireless network can fluctuate and be hard to predict. The switch matrix allows the capacity of the wireless network to be balanced to the base stations by modifying the coverage area of individual sectors to provide the optimum quality of service to users.

4. Fault recovery- The addition of a switch matrix endows the network with much greater flexibility to recover from fault conditions. For example, the failure of a base station can be recovered remotely and immediately by reallocating its remote antennas to alternative base stations.

5.Planned maintenance- In a similar fashion to fault recovery, the network configuration can be modified to allow for planned maintenance.

6. Network evolution- New antenna infrastructure is not required for the deployment of new services or capacity.

6 Service introduction-can be achieved with the installation of a single new base station in the central location, and the coverage and pace of the subsequent roll-out can be controlled remotely through the switch matrix. The purchase of additional new base stations is only required when greater capacity is needed.

2.9. RoF For Ultra Wide Band Radio:

There is demand for wireless broadband services to access bandwidth intensive applications such as audio/video streaming. Pulsed Ultra Wide Band (UWB) radio is one such technology that can support these high-speed applications. However, regulatory UWB transmission power restricts coverage to a small area. Large number of base stations will be needed to provide wide coverage area for mobile users. Radio-over-Fiber (RoF) network is an attractive option in offering the necessary linkages between UWB radio base stations and their central office. RoF network is a cost effective way in distributing UWB signals between central office and its remote base stations. New advances in multimode fiber modal bandwidth are allowing new techniques in signal distribution for microwave photonics applications.

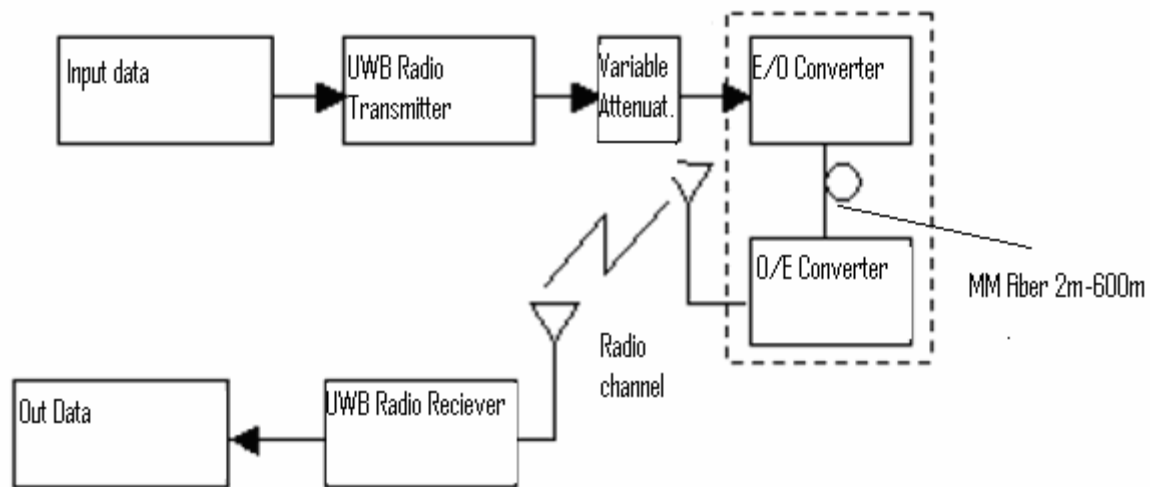


Figure 2.12 RoF Architecture for UWB Radio.

The figure above shows a typical UWB Radio employing the RoF link. Here the use data is sent to the UWB Radio transmitter. This radio signal is then sent to the E/O converter where the radio signal modulates the Laser diode and this composite signal is sent over the fiber channel.

3. Effect of the Laser and RF Oscillator Linewidths

3.1 Introduction

The volume of data traffic is ever increasing due to the demand of subscribers for voice, data, and multimedia services that require the access network to support high data rates at any time and in any place expensively. For satisfying the demands, wideband communication systems are necessary in both wired link and wireless link. Radio-over-fiber (RoF) systems have been good candidates for broadband services since an optical fiber provides low loss and large bandwidth and a radio signal enables the mobility and easy access. Generally, ROF systems transmit an optically modulated radio frequency (RF) signal from a central office (CO) to a base station (BS) via an optical fiber. The RF signal recovered using a photo detector (PD) at the BS arrives at a user terminal (UT) through a wireless channel. This architecture provides a cost-effective system since any RF oscillator is not required at the BS. However, the performance of RoF systems depends on the method used to generate the optically modulated RF signal, power degradation due to fiber chromatic dispersion, nonlinearity due to an optical power level, and phase noises from a laser and an RF oscillator. Therefore, it has been a matter of concern and interest to investigate parameters that degrade the performance of RoF systems and how to enhance the performance cost effectively.

There are two techniques to generate the optically modulated RF signal: direct and external modulation. The direct modulation scheme is simple but suffers from a laser-frequency chirp effect, and this chirp effect results in severe degradation of the system performance. However, this can be eliminated by using the external-modulation scheme instead of the direct modulation scheme. Although the external-modulation scheme is employed, the conventional optical double sideband (ODSB) signal can degrade the received RF signal power due to fiber chromatic dispersion drastically. For overcoming the power degradation, an optical single sideband (OSSB) signal, generated by using a

phase shifter and a dual-electrode (DE) Mach–Zehnder modulator (MZM), is employed. In addition to these two effects, the nonlinearity of an optical fiber can give a large penalty on the long-haul transmission and multi channel system using a high-power signal. For the high-power transmission, the nonlinear effect should be managed by utilizing a modulation format, and by controlling the launched power level. The nonlinear effect, however, can be negligible in short and low optical power (< 0 dBm), especially for a single channel transmission.

Unlike those parameters, phase noise is one of the practical and decisive factors in high-quality services that require high signal-to-noise ratio (SNR), because it results in a bit error rate (BER) floor in a high SNR value. This phenomenon is serious to RoF systems because the purpose of RoF systems is to provide a service of high data rate and high quality, which require a large SNR. Thus, the system performance can be more sensitive to the phase noise in these services.

The influence of the phase noise on optical communication systems has been investigated. Kitayama[6] analyzed the system performance for an ODSB signal including laser phase noise and suggested how to compensate the differential delay by using a dispersion-compensating fiber (DCF). He focused on how to compensate fiber chromatic dispersion for the ODSB signal experimentally and analytically rather than analyze the effect of the phase noise on the performance in detail. Salz analyzed the performance of coherent optical systems with laser phase noise by utilizing a Wiener process, since coherent detection provides better sensitivity than that of direct detection, while direct detection has a simple structure.

Gallion analyzed the power spectral density (PSD) function of a photocurrent incorporating the laser phase noise in detail. Gliese[7] applied the result in to the evaluation of a carrier-to-noise ratio (CNR) penalty and an rms phase noise at the receiver due to the laser linewidth and fiber chromatic dispersion in a remote heterodyne detection (RHD) system [10]. For the tolerance to fiber chromatic dispersion, dual correlated lasers were employed to generate An OSSB signal. In, the CNR penalty due to the laser linewidth is negligible in a narrow laser linewidth and small differential delay (< 100 ps) while the CNR penalty is quite large in a broad laser linewidth and large differential delay. In spite of numerous papers about the performance of RoF systems

with the phase-noise effect, there is still a need to evaluate the performance of RoF systems on a practical optical length to design a cost-effective system that does not require an additional optical amplifier. Conventional cellular systems use a microcell for the high density of users in a suburban area and a macrocell in the case when the radius is from 8 to 24 km.

Furthermore, the commercially used frequency for multimedia service is only several gigahertz. In such an environment, the phase noise of the RF signal can be dominant rather than the laser linewidth, while the laser phase noise almost does not influence the performance degradation if the carrier frequency is not quite high (< 50 GHz).

Thus, more specific analysis of RoF systems, including the phase noise of the RF signal is necessary.

3.2. RoF System Architecture

The overall downlink architecture of the RoF system is shown in Figure 1 above in chapter 1. Data are converted by the RF oscillator and optically modulated by a laser diode (LD) with an MZM in a CO. The output signal of the MZM is transmitted via a standard single-mode fiber (SSMF) and detected by a PD to generate the photocurrent at a BS that is simple and compact. The photocurrent goes through a band pass filter (BPF) and an amplifier to be launched into a wireless channel in the BS. The wireless channel makes signals vulnerable to amplitude and phase distortion. A UT amplifies and filters the received signal to detect the transmitted RF signal. Finally, the data are extracted through RF demodulation.

Fig. above describes the optical link in detail. An OSSB signal is generated by using an MZM and a phase shifter. An RF signal from an oscillator is split by a power splitter and a 90° phase shifter. This RF signal is optically modulated by the LD with an MZM. The optically modulated signal is transmitted to the PD and the photocurrent corresponding to the transmitted RF signal is extracted by the BPF. First, the optical signals from the laser and the RF oscillator are modeled as follows:

$$\begin{aligned} x_{LD}(t) &= A \cdot \exp j(\omega_{LD}t + \Theta_{LD}(t)) \\ x_{RF}(t) &= V_{RF} \cdot \exp j(\omega_{RF}t + \Theta_{RF}(t)) \end{aligned} \quad (1)$$

Where A and V_{RF} define amplitudes from the LD and the RF oscillator, ω_{LD} and ω_{RF} define angular frequencies of the signals from the LD and the RF oscillator, and $\Phi_{LD}(t)$ and $\Phi_{RF}(t)$ are phase-noise processes.

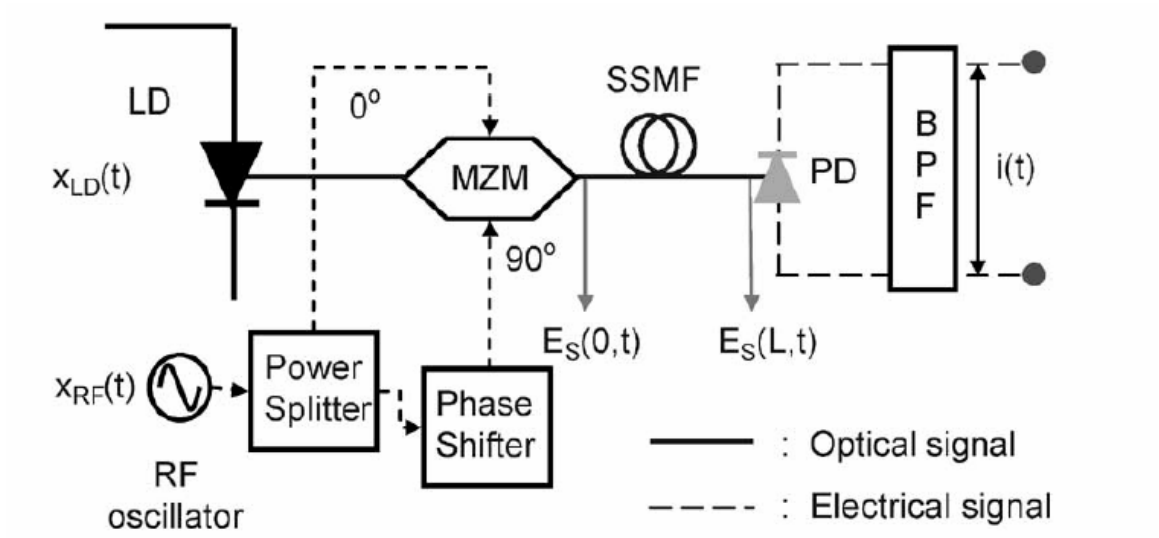


Figure 3.1 Optical Link in RoF

Unlike the phase-noise process from the laser, the phase-noise process $\Phi_{RF}(t)$ from the RF oscillator is difficult since the spectrum consists of a Flicker frequency, a white frequency noise, and a white phase noise.

After optically modulating $x_{RF}(t)$ by $x_{LD}(t)$ with a DE MZM, the output signal of the DE MZM is represented as:

$$E(0,t) = \frac{L_{MZM} \cdot x_{LD}(t)}{\sqrt{2}} \left\{ \begin{aligned} &\exp j\left[\gamma\pi + \frac{\pi}{V\pi} \cdot \frac{x_{RF}(t)}{\sqrt{2}}\right] \\ &+ \exp j\left[\frac{\pi}{V\pi} \cdot \frac{x'_{RF}(t)}{\sqrt{2}}\right] \end{aligned} \right\} \quad (2)$$

$$E(0,t) = \frac{L_{MZM}}{\sqrt{2}} \left\{ \exp j[\omega_{LD}t + \gamma\pi + \Theta_{LD}(t)] + \alpha\pi \cos(\omega_{RF}t + \Theta_{RF}(t)) + \exp j(\omega_{LD}t + \Theta_{LD}(t) + \alpha\pi \cos(\omega_{RF}t + \Theta_{RF}(t))) \right\}$$

Eqn (1)

where $\tilde{x}_{RF}(t)$ denotes the phase-shift version of $x_{RF}(t)$, $\gamma(= V_{dc}/V\pi)$ and $\alpha(= V_{RF}/\sqrt{2}V\pi)$ define a normalized dc and ac value, $V\pi$ is the switching voltage of the DE MZM, L_{MZM} is the insertion loss of the DE MZM, and θ is the phase shift by the phase shifter. Note that the input RF signals into the DE MZM are $x_{RF}(t)/\sqrt{2}$ and $\tilde{x}_{RF}(t)/\sqrt{2}$ rather than $x_{RF}(t)$ and $\tilde{x}_{RF}(t)$

because the input RF signal is 3-dB attenuated by utilizing the power splitter. By controlling the phase shifter, the output signal can be the OSSB or the ODSB signal. Among the two signals, only the OSSB signal will be dealt with in this paper since the ODSB signal suffers from fiber chromatic dispersion severely and requires double bandwidth than that of the OSSB signals.

For generating the OSSB signal, θ and γ are set to $\pi/2$ and $1/2$, respectively. By using (4) and the mentioned conditions, the OSSB signal at the DE MZM can be modeled as follows:

$$E(0,t) = A.L_{MZM} \cdot \left\{ J_0(\alpha\pi) \cdot \exp j[\omega_{LD}t + \Theta_{LD}(t) + \frac{\pi}{4}] - \sqrt{2}J_1(\alpha\pi) \cdot \exp j(\omega_{LD}t + \Theta_{LD}(t) + \omega_{RF}t + \Theta_{RF}(t)) \right\}$$

(5)

It is assumed that high-order components of the Bessel function can be negligible since the value of $\alpha\pi$ in the Bessel function is very small due to the fact that $V\pi \gg V_{RF}$ in general. The output signal at the DE MZM is transmitted via the SSMF experiencing different group delays, due to the fiber chromatic dispersion, at a different wavelength. After the transmission of L_{fiber} -km SSMF, the signal at the end of the SSMF becomes:

$$E(L,t) = A.L_{MZM} \cdot L_{add} \cdot 10^{\frac{-\alpha_{fiber}L_{fiber}}{20}} \cdot J_0(\alpha\pi) \cdot \left\{ \exp j(\omega_{LD}t + \Theta_{LD}(t - \tau) - \phi_1 + \frac{\pi}{4}) - \frac{\sqrt{2}J_1(\alpha\pi)}{J_0(\alpha\pi)} \cdot \exp j(\omega_{LD}t + \omega_{RF}t + \Theta_{LD}(t - \tau_+) + \Theta_{RF}(t - \tau_+) - \phi_2) \right\}$$

(6)

where L_{add} denotes an additional loss in the optical link, α_{fiber} is the SSMF loss, L_{fiber} is the transmission distance of the SSMF, and τ_0 and τ_+ define group delays for a center

angular frequency of ω_{LD} and an upper sideband frequency of $\omega_{LD} + \omega_{RF}$. ϕ_1 and ϕ_2 are phase-shift parameters for specific frequencies due to the fiber chromatic dispersion.

3.3. CNR Penalty Analysis

In this section the system performance based on the photocurrent at the PD is studied. For the evaluation of the performance of the RoF system, a CNR is utilized because it is simple and is a good parameter for measuring the system performance by employing the ratio between the carrier power and the noise power. The CNR of the photocurrent is calculated by using an autocorrelation function and a PSD function. The CNR penalty, which is defined as the ratio between the CNR value and the reference CNR value is also studied. The CNR penalty, as well as the CNR, is also important and practical in a real system because, generally, the derived CNR value itself is not same as the real CNR value. However, the CNR penalty can show the effect of the specific parameter on the system performance as the value of the parameter is changed. To evaluate the CNR and the CNR penalty, the autocorrelation function and the PSD of the photocurrent are utilized. By using a square-law model, the photocurrent $i(t)$ can be obtained from (6) as follows:

$$\begin{aligned} i(t) &= \Re |E_s(L, t)|^2 \\ i(t) &= \Re^2 \cdot A^2 [B + \cos(\omega_{RF}t + \Theta_{LD}(t - \tau_+) - \Theta_{LD}(t - \tau_0) + \Theta_{RF}(t - \tau_+) - \phi_2 + \phi_1)] \end{aligned} \quad (7)$$

Where

$$\begin{aligned} A_1 &= A \cdot L_{MZM} \cdot L_{add} \cdot 10^{\frac{-\alpha_{fiber} L_{fiber}}{20}} \cdot J_0(\alpha\pi) \\ \alpha &= \frac{\sqrt{2} J_1(\alpha\pi)}{J_0(\alpha\pi)} \\ B &= 1 + \alpha_1^2 \end{aligned}$$

Where R defines the responsivity of the PD and $|E(L, t)|^2$ is the Square-law detection. From (7), the autocorrelation function $R_I(\tau)$ is obtained as:

$$R_I(\tau) = \langle i(t) \rangle \cdot \langle i(t + \tau) \rangle \quad (8)$$

$$\frac{R_I(\tau)}{\mathfrak{R}^2 \cdot A^4} = B^2 + \begin{cases} 2 \cdot \alpha^2 \cdot \cos(\omega_{RF} \tau) \exp(-2\gamma_l |\tau|) & |\tau| \leq \tau_1 \\ 2 \cdot \alpha^2 \cdot \cos(\omega_{RF} \tau) \exp(-2\gamma_{LD} \tau_1 - 2\gamma_l |\tau|) & \text{otherwise} \end{cases} \quad (9)$$

Where $\Delta\nu_{LD}$ and $\Delta\nu_{RF}$ are the linewidths for the laser and the RF oscillator, respectively, $2\gamma_{LD}$ ($= 2\pi\Delta\nu_{LD}$) and $2\gamma_{RF}$ ($= 2\pi\Delta\nu_{RF}$) define the angular full-linewidth at half maximum (FWHM) of the Lorentzian shape for the laser and the RF oscillator, respectively, and $2\gamma_l$ is related to the total linewidth. Note that the $2\gamma_l$ is given not as $2\pi\Delta\nu_{LD} + 2\pi\Delta\nu_{RF}$ but $2\pi\Delta\nu_{LD} + \pi\Delta\nu_{RF}$. $\tau_1 = (\tau_+ - \tau_0)$ is the differential delay due to the fiber chromatic dispersion and is dependent on the wavelength λ , the carrier frequency f_{RF} , the fiber chromatic dispersion D , and the optical transmission distance L_{fiber} . It is given by [2].

$$\tau_1 = D \cdot L_{fiber} \cdot \lambda^2 \cdot \frac{f_{RF}}{c} \quad (10)$$

I have also studied the relation between the fiber chromatic parameter D and CNR Penalty for different laser linewidths. The results are shown in the fig. 11 below.

The PSD function of the photocurrent is given by the Fourier transform of (8). The shot noise term at the PD is omitted here since the noise power can be evaluated by the product of bandwidth and noise density level. The PSD function $S_I(f)$ can be written as:

$$\begin{aligned} S_I(f) &= F \langle R_I(\tau) \rangle \\ \frac{S_I(f)}{\mathfrak{R}^2 \cdot A^4} &= B^2 \delta(f) + \frac{2\gamma_{RF} \alpha^2 \cdot e^{-2\tau_1 \gamma_l} \cos[2\pi(f - f_{RF})\tau_1]}{\gamma_{RF}^2 + [2\pi(f - f_{RF})]^2} \\ &+ \frac{4\alpha^2 \cdot e^{-2\gamma_l \tau_1}}{(2\gamma_l)^2 + [2\pi(f - f_{RF})]^2} \cdot \{\gamma_l \alpha^2 \cdot e^{2\tau_1 \gamma_l} - \gamma_l \cos[2\pi(f - f_{RF})\tau_1]\} \\ &- \frac{4\pi \cdot \gamma_{LD}(\gamma_{LD} + \gamma_{RF})(f - f_{RF})}{\gamma_{RF}^2 + [2\pi(f - f_{RF})]^2} \cdot \sin[2\pi(f - f_{RF})\tau_1] + G(f + f_{RF}) \end{aligned} \quad (11)$$

where F denotes Fourier transform and $G(f + f_{RF})$ is

$$\begin{aligned}
G(f + f_{RF}) &= \frac{2\gamma_{RF}\alpha_1 e^{-2\tau_1\gamma_l} \cos[2\pi(f + f_{RF})\tau_1]}{\gamma_{RF}^2 + [2\pi(f + f_{RF})]^2} \\
&+ \frac{4\alpha_1^2 e^{-2\gamma_l\tau_1}}{(2\gamma_l)^2 + [2\pi(f - f_{RF})]^2} \cdot \{\gamma_l\alpha_1 e^{2\tau_1\gamma_l} - \gamma_l \cos[2\pi(f + f_{RF})\tau_1]\} \\
&- \frac{4\pi\gamma_{LD}(\gamma_{LD} + \gamma_{RF})(f + f_{RF})}{\gamma_{RF}^2 + [2\pi(f + f_{RF})]^2} \cdot \sin[2\pi(f + f_{RF})\tau_1] \}
\end{aligned} \tag{11}$$

The first term of (11) represents a dc component, the second and third is the broadening effects due to the fiber chromatic dispersion and the linewidths of the laser and the RF oscillator. The $\delta(f)$ is defined as follows:

$$\delta(f) = \frac{1}{\pi} \lim_{a \rightarrow 0} \frac{a}{a^2 + f^2} \tag{12}$$

By using (11), the received RF carrier power P_I is approximately represented as follows

$$P_I = 2 \int_{f_{RF} - \frac{B_{RF}}{2}}^{f_{RF} + \frac{B_{RF}}{2}} S_I(f) df$$

$$\begin{aligned}
P_I &= \frac{4\Re A^4 \alpha_1^2}{\pi} \left\{ (1 - e^{-2\gamma_l\tau_1}) \tan^{-1} \left(\frac{\pi B_{RF}}{2\gamma_l} \right) + e^{-2\gamma_l\tau_1} \cdot \tan^{-1} \left(\frac{\pi B_{RF}}{2\gamma_{RF}} \right) \right\} \\
&\text{for } -\pi B_{RF}\tau_1 \ll 1 \\
&\text{and}
\end{aligned} \tag{13}$$

$$\begin{aligned}
&\text{for } -2\gamma_l\tau_1 \ll \gamma_{RF} \\
P_I &= \frac{4\Re A^4 \alpha_1^2}{\pi} \cdot e^{-2\gamma_l\tau_1} \tan^{-1} \left(\frac{\pi B_{RF}}{2\gamma_l} \right)
\end{aligned}$$

In (13), the last condition, $2\gamma_l\tau_1 \ll 1$ and $\gamma_l \ll \gamma_{RF}$, is reasonable because the laser linewidth is much greater than the RF-oscillator linewidth and the fiber length is usually less than a few tens of kilometers in RoF systems. Note that the coefficient 2 of (13) is due to the real and imaginary spectrum. The cos and sin terms in (11) are approximately equal to 1 and 0 in the integrand when $\pi B \tau_1 \ll 1$ is satisfied. The received RF carrier power is a function of the differential delay τ_1 , the linewidths of the laser and the RF

oscillator, and the bandwidth of the electrical filter B_{RF} . The ratio between the bandwidth and the linewidth of the RF oscillator is one of the dominant parameters for the carrier power. Practical systems employ various types of bandwidth as the required power, such as half-power bandwidth, fractional-power containment bandwidth (99% of signal power), etc. For evaluating the total RF power excluding dc power, we utilize (9) as follows:

$$\begin{aligned} P_t &= R_t(0) - \Re^2 \cdot A^4 \cdot B^2 \\ &= 2\Re^2 \cdot A^4 \cdot \alpha_1^2 \end{aligned} \quad (14)$$

By using (14), we define the ratio p between the total carrier power and the required power as follows:

$$\begin{aligned} p &= \frac{P_l}{P_t} \\ &\text{for } 2\gamma_t\tau_1 \ll \gamma_{RF} \text{ and } \gamma_t \ll \gamma_{RF} \\ p &\approx \frac{2}{\pi} \cdot e^{-2\gamma_t\tau_1} \tan^{-1}\left(\frac{\pi B_{RF}}{2\gamma_{RF}}\right) \end{aligned} \quad (15)$$

From (15), the required bandwidth for the p ratio is obtained as:

$$B_{RF} = \frac{\gamma_{RF}}{\pi} \cdot \tan\left(\frac{\pi}{2} e^{2\gamma_t\tau_1} p\right) \quad (16)$$

The required bandwidth increases as we need more received signal power. Note that the required bandwidth for a specific received carrier power is dominantly dependent on the phase noise from the RF oscillator rather than that from the laser for $2\gamma_t\tau_1 \ll 1$ and $\gamma_t \ll \gamma_{RF}$. However, when $2\gamma_t\tau_1$ is not enough to be ignored and $e^{2\gamma_t\tau_1} p$ approaches 1, B_{RF} will be infinite.

By using (13) and (16), the CNR penalty induced by the differential delay from the fiber chromatic dispersion and the linewidths from the laser and the RF oscillator is found as

$$CNR = \frac{\text{Carrier Power}}{\text{Noise Power}}$$

$$\begin{aligned}
CNR &= \frac{P_I}{2B_{RF} \cdot \frac{N_0}{2}} \\
&= \frac{\Re A^4 \alpha^2 p}{N_0 \frac{\gamma_{RF}}{\pi} \frac{\gamma_{RF}}{\pi} \cdot \tan\left(\frac{\pi}{2} e^{2\gamma\tau_1} p\right)}
\end{aligned} \tag{17}$$

Note that $2B_{RF}$ is utilized instead of B_{RF} since P_I is the received RF signal power in both real and imaginary parts and noise power must be evaluated in the same manner. From (17), we investigate the CNR penalty due to the linewidths, the differential delay, and the filter type. If CNR_0 is defined as a Reference CNR, the CNR penalty ΔCNR is represented as:

$$\begin{aligned}
\Delta CNR &= 10 \log_{10}\left(\frac{CNR_0}{CNR}\right) \\
\Delta CNR &= 10 \log_{10}\left(\frac{p_0 \gamma_{RF} \cdot \tan\left(\frac{\pi}{2} e^{2\gamma\tau_1} p\right)}{p \cdot \gamma_{RF_0} \cdot \tan\left(\frac{\pi}{2} e^{2\gamma\tau_1} p_0\right)}\right) \text{--- eqn(18)}
\end{aligned}$$

For calculating the CNR_0 , we set p_0 to 0.5 as a half-power bandwidth filter, γ_{RF_0} to π , which means a 1-Hz linewidth of the RF oscillator, and zero laser linewidth. The CNR penalty ΔCNR depends on p , the linewidths, and the differential delay. Firstly, we investigate the effect of p and γ_{RF} on the CNR Penalty under a 10-km fiber, 30-GHz RF carrier, fiber dispersion parameter D ($= 17$ ps/nm km), and 1550-nm laser with zero linewidth. From [2] we obtain the relation between group delay and the fiber chromatic dispersion parameter D as:

$$\tau_1 = D \cdot L_{fiber} \cdot \lambda^2 \cdot \frac{f_{RF}}{c} \tag{19}$$

I have also analysed the relation between the fiber chromatic parameter D and CNR Penalty for different laser linewidths. The results are shown in the fig. 11 below.

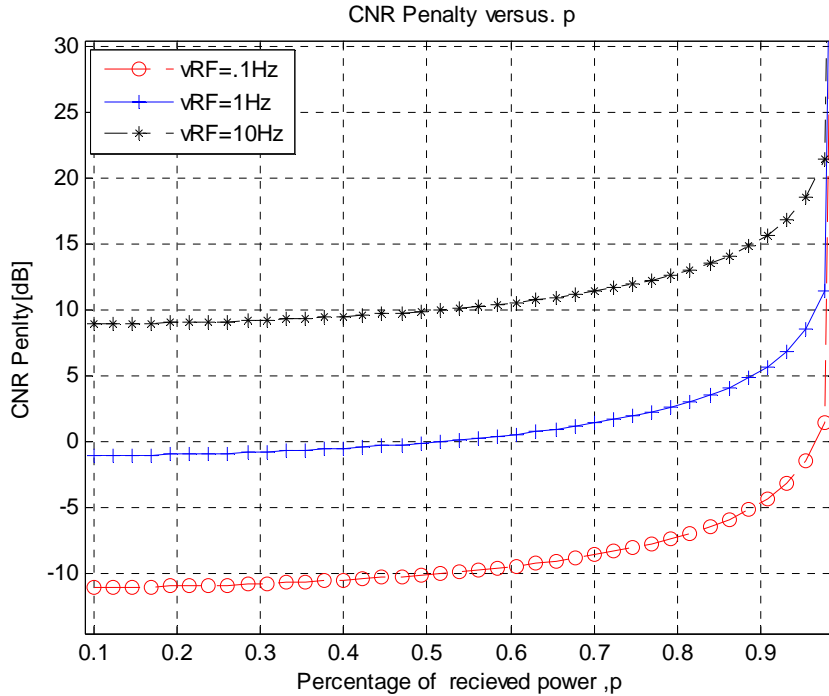


Fig 3.2 Δ CNR as a function of the percentage of the received power p and linewidth of the RF oscillator as compared to the half-power bandwidth p_0 and 1-Hz $\Delta\nu_{RF0}$.

Δ CNR is sketched in Fig. 3. The linewidth of the RF oscillator has been swept from 0.1 to 10 Hz. usually; the linewidth of the RF oscillator is less than 1 Hz [6]. However, here only example over 1 Hz is studied, as a practically cost-aware RF oscillator. As the result, in Fig., Δ CNR consists of the RF-oscillator-linewidth effect γ_{RF} and the ratio p . The effect of γ_{RF} is linearly proportional to Δ CNR, as shown in (18) and Fig. 3. The linear proportion means that Δ CNR increases 10 dB, which is equivalent to ten times the increment of γ_{RF} . Δ CNR also increases as p becomes large since the increment of the noise power is greater than that of the received signal power as the bandwidth increases. Thus, the bandwidth should be considered carefully for $p > 90\%$, since the CNR penalty increases drastically over the point as a result. For example, the CNR penalty of $p = 0.99$ is 15.1 dB as compared to $p = 0$. We can also obtain minus CNR penalty, which means a gain in $p < 0.5$ because the reference ratio is $p_0 = 0.5$. The received RF signal power, however, will decrease less than 50%. Thus, the minimum required power to detect the signal should be carefully considered before we choose the filter bandwidth. Another parameter that affects Δ CNR is the laser linewidth.

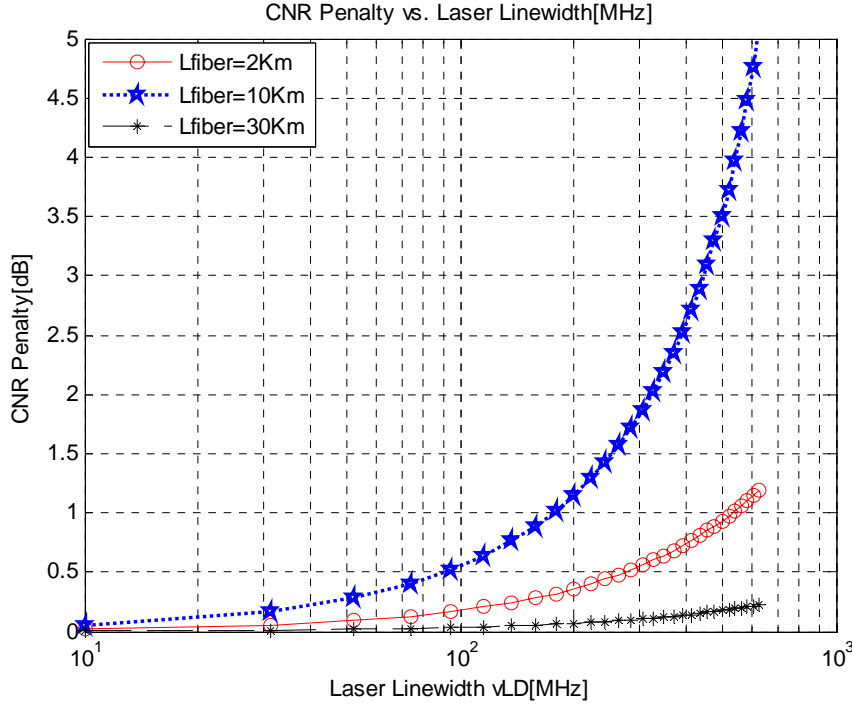


Fig 3.3 ΔCNR as a function of the laser linewidth $\Delta\nu_{LD}$ and fiber transmission distance L_{fiber} as compared to the zero laser linewidth

The result of the laser-linewidth effect is described in Fig. 4. Here the laser linewidth is swept from 10 to 624 MHz since 10 and 624 MHz are typical linewidth values of a distributed-feedback (DFB) laser and a Fabry–Pérot (FP) laser. ΔCNR exponentially increases as the laser linewidth. Therefore, the RoF system relatively suffers from ΔCNR for a long transmission, such as 30 km, while ΔCNR is almost not changed ($=0.22$ dB) Even for the FP laser in the short-transmission case ($=2$ km). We can confirm that the FP laser can be used in a practical microcell boundary because the radius of the microcell is from 0.2 to 1 km [20].

From ΔCNR in (18), we can take into account the CNR penalty in detail. In order to investigate the effect of the linewidth, we set the $p(=PI/Pt)$ value as 0.5 in any situation, and it means that the same type of filter, such as the half-power bandwidth, is utilized for all cases. For the 1550-nm laser, 30-GHz carrier frequency, and each distance of the 2-, 10-, and 30-km SSMFs, the CNR penalty with respect to the reference parameters of the

1-Hz linewidth of the RF oscillator is shown in Fig. 5. We sweep the linewidth of the RF oscillator from 0.1 to 10 Hz according to different laser linewidths. As the results show, the phase noise from the RF oscillator gives a constant effect, as in Fig. 3, while the CNR penalty due to the laser linewidth increases exponentially as the product of the laser linewidth and the differential delay.

For a short distance, the phase noise from the RF oscillator is the dominant factor of the CNR penalty. The CNR penalty due to the laser linewidth increases dramatically over a specific distance. Therefore, the laser linewidth should be selected carefully in a long-haul transmission since the large differential delay and large laser linewidth cause a serious CNR penalty. For example, the CNR penalty of the RF oscillator due to the increment of the phase noise from 0.1 to 10 Hz is around 20 dB in any case, while the CNR penalties due to the laser linewidth for 624 MHz are 0.22, 1.2, and 4.9 dB in 2-, 10-, and 30-km SSMFs. This means that we can employ a cheap laser such as the FP laser in the RoF system in microcell and macrocell without a severe CNR penalty.

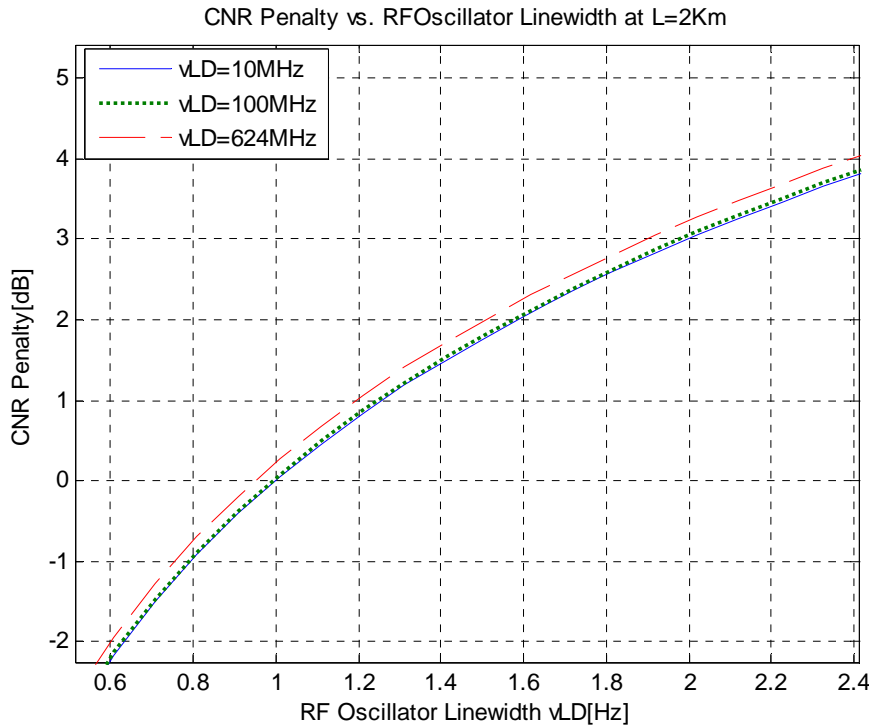


Fig 3.4 Δ CNR as a function of the RF linewidth $\Delta\nu_{RF}$ and laser line width $\Delta\nu_{LD}$ at $L_{fiber}=2$ Km

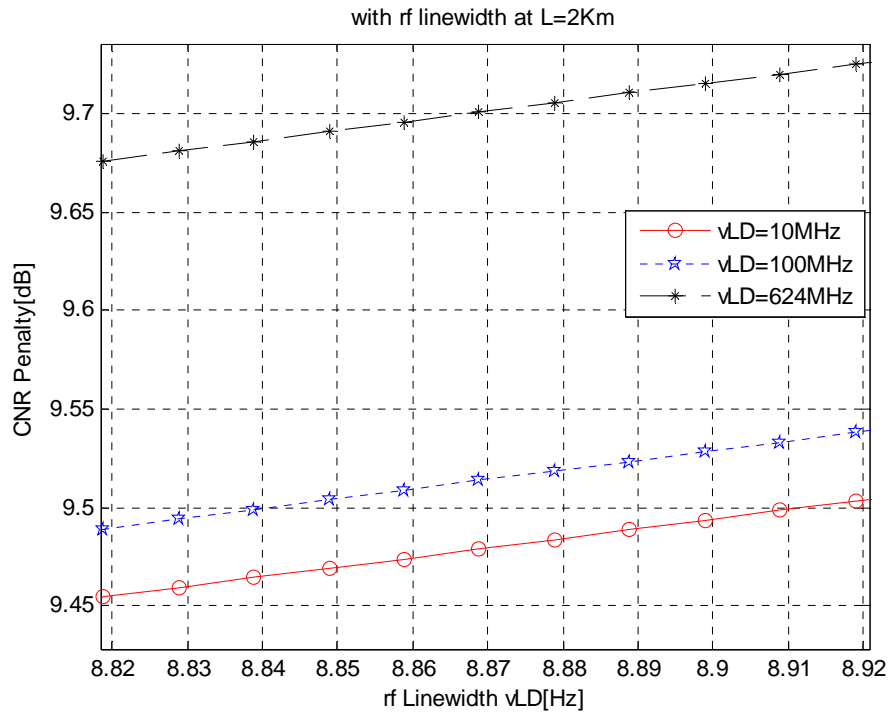


Fig 3.5 Δ CNR as a function of the RF linewidth $\Delta\nu_{RF}$ and laser line width $\Delta\nu_{LD}$ at Lfiber =2Km expanded view

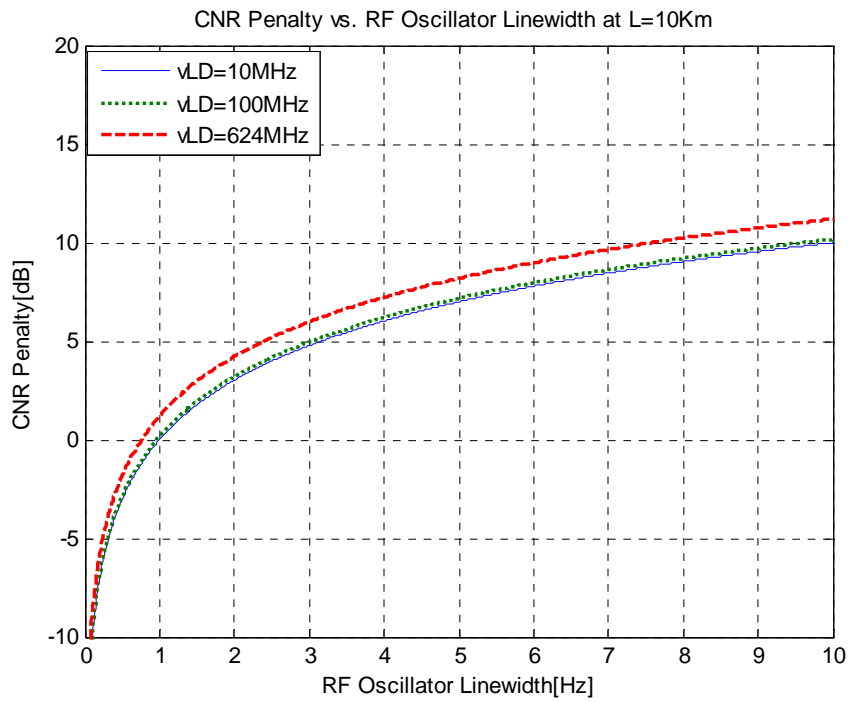


Fig 3.6 Δ CNR as a function of the RF linewidth $\Delta\nu_{RF}$ and laser line width $\Delta\nu_{LD}$ at Lfiber =10Km

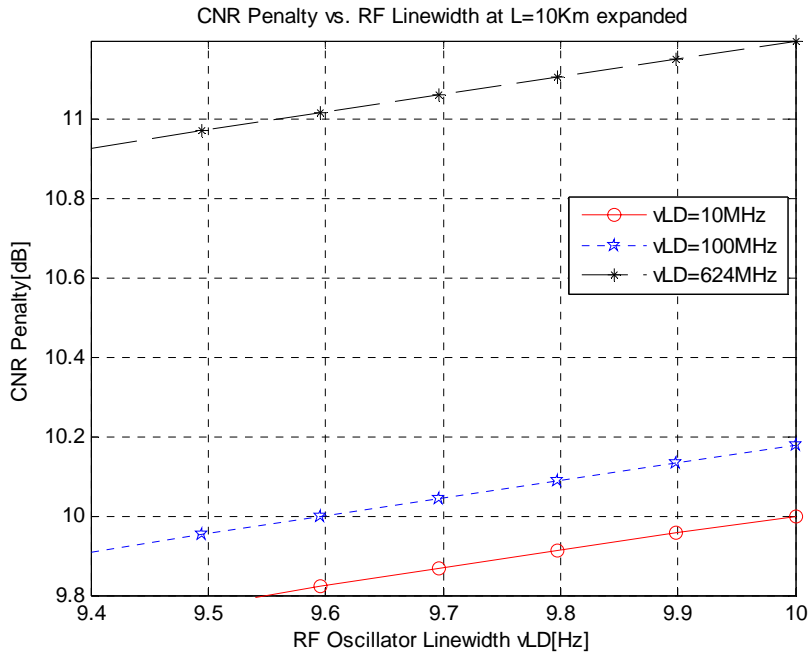


Fig3.7 Δ CNR as a function of the RF linewidth $\Delta\nu_{RF}$ and laser line width $\Delta\nu_{LD}$ at $L_{fiber} = 10\text{Km}$ expanded view

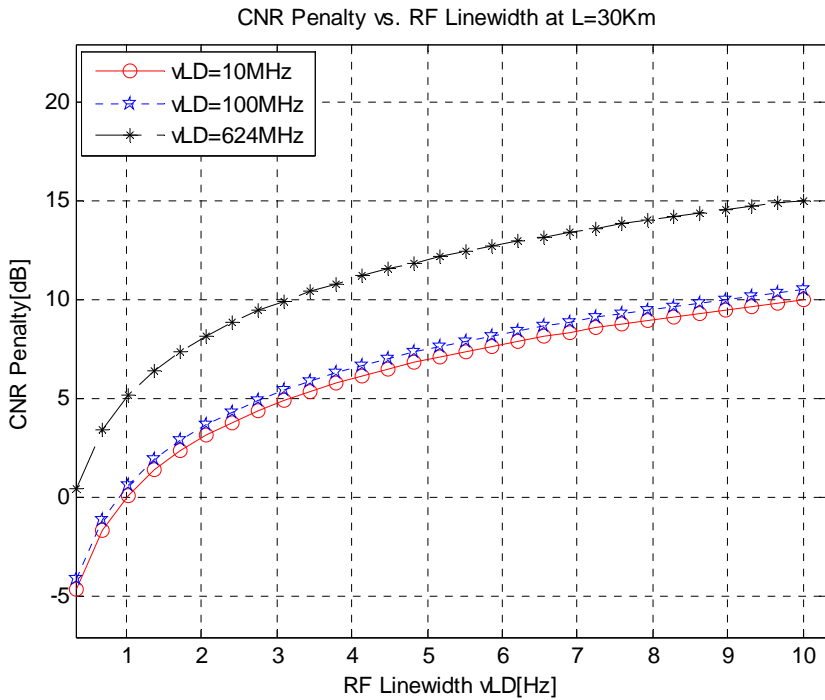


Fig 3.8 Δ CNR as a function of the RF linewidth $\Delta\nu_{RF}$ and laser line width $\Delta\nu_{LD}$ at $L_{fiber} = 30\text{Km}$

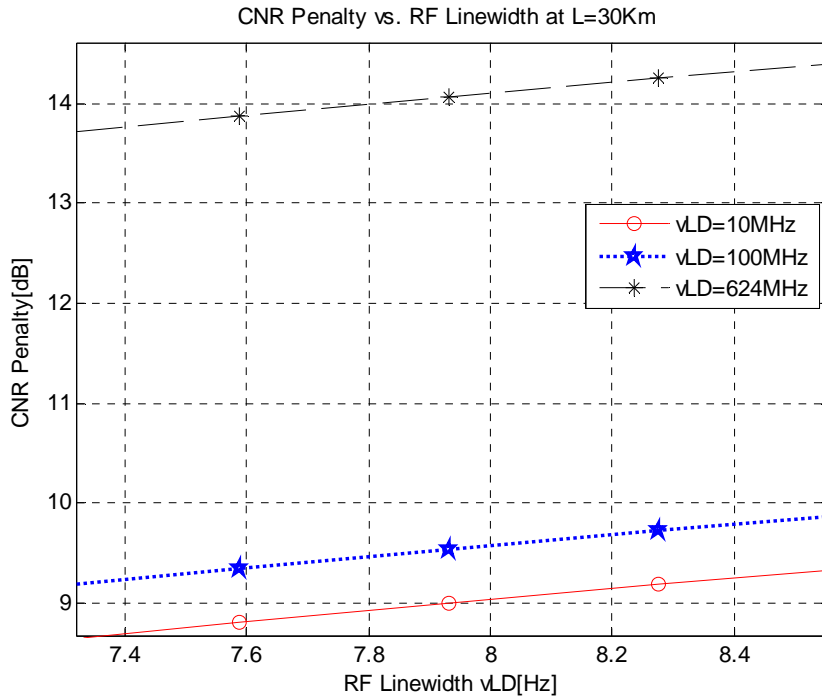


Fig 3.9 Δ CNR as a function of the RF linewidth $\Delta\nu_{RF}$ and laser line width $\Delta\nu_{LD}$ at $L_{fiber} = 30$ Km expanded view

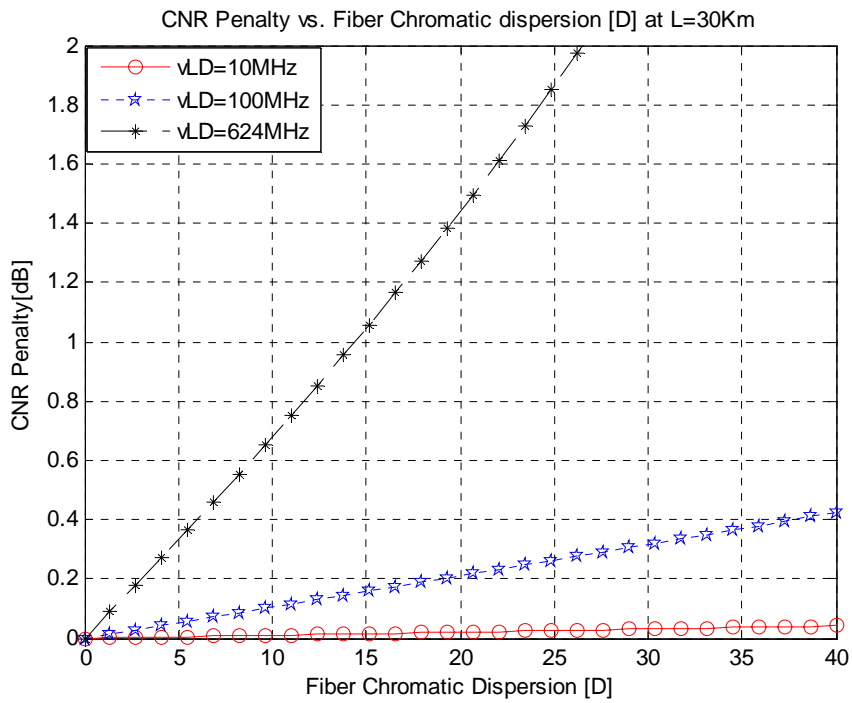


Figure 3.10 ΔCNR as a function of the Chromatic Dispersion D and laser line width $\Delta\nu_{LD}$ at $L_{\text{fiber}}=2\text{Km}$

Through these results, we can notice that, by using the external-modulation scheme, the phase noise of the RF signal influences the system performance much more than the phase noise from the laser in direct detection.

3.4. Discussion

The CNR penalty due to the limits of the fiber chromatic dispersion in the standard single-mode fiber (SSMF) and the phase noises of the laser and the radio frequency (RF) oscillator in the radio-over-fiber (RoF) system. In order to investigate the CNR penalty, we evaluate the power spectral density (PSD) function, and our PSD function is identical with the previous result in [8], when the phase noise of the RF oscillator is 0. A practical laser having nonzero linewidth induces CNR penalty by the multiplication with nonzero differential delay

in the RoF system that employs external modulation with a dual-electrode Mach–Zehnder modulator (DE-MZM) and direct detection. However, the CNR penalty due to the laser linewidth is much less than the CNR penalty due to the RF-oscillator linewidth.

The CNR penalty comes from the power degradation due to phase noises and the differential delay caused by fiber chromatic dispersion. The filter bandwidth at an electrical receiver should be selected carefully considering tradeoff between the CNR penalty and required signal power ratio p , especially for $p > 0.9$, since the increase of bandwidth causes the increase of noise power. The CNR penalty for the use of a 99% bandwidth filter is 15.1 dB, as compared to the case using the half-power bandwidth.

Moreover, the linewidth of the RF oscillator gives an additional 20-dB CNR penalty for the increment of the linewidth from 0.1 to 10 Hz. It is noteworthy that the remaining challenge of these high-stability RF-modulated optical sources is known to be the reduction of the phase noise (spectral broadening). We considered a pessimistic, yet practically cost aware approach. For the power degradation due to the phase noises, the CNR penalty increases exponentially as the multiplication of the linewidths and the differential delay. The FP laser can be applied into a practical system since the CNR

penalty due to the FP laser linewidth is only 0.22 dB in a microcell (2 km) even though it becomes relatively severe in a long distance (30 km). From these observations, we can figure out that the CNR penalty is more sensitive to the phase noise from the RF oscillator rather than that from the laser in a relatively short transmission distance (< 10 km). These results are reasonable for the direct-detection scheme based on the external modulation in a short transmission distance. The RF carrier signal at the photodetector (PD) is generated by beating, or “multiplying,” the signal components with each other in the direct detection. When the external-modulation scheme is employed, the initial phase-noise effect due to the Laser linewidth for the frequency components at ω_{LD} and $\omega_{LD} + \omega_{RF}$ are almost kept at the end of an optical fiber if the transmission distance is relatively short. This negligible change of the phase between $\exp j(\omega_{LD})$ and $\exp j(\omega_{LD} + \omega_{RF})$ can almost be canceled after beating each other at the PD in a short transmission, since the signals for each frequency component experience almost the same group delay. In that case, the phase noise from the RF oscillator influences the system performance much more than that from the laser source. However, the long-haul transmission is different because the initial phase difference is not maintained at the end of the optical fiber anymore. The observed linewidth due to the laser at the PD will be twice that of an initial laser linewidth $\Phi_{LD}(t)$ since the differential delay is much greater than the coherence time. Therefore, the phase noise processes of $\Phi_{LD}(t)$ and $\Phi_{LD}(t + \tau_1)$ are completely uncorrelated [9]. In that case, the system performance will suffer from the laser linewidth in a long-haul case seriously while the laser-linewidth effect can be ignored in a short transmission. Through these observations, it can be guessed that the performance of a coherent detection that utilizes another laser as a local oscillator (LO) can be more sensitive to the laser linewidth, because the phase noise from an LO is added into the received signal in the coherent detection.

In conclusion, the bandwidth of an electrical filter at the receiver should be carefully chosen considering minimum required signal power ratio p and CNR penalty at the same time. The externally modulated OSSB signal incorporating direct detection at the receiver is tolerable for the CNR penalty due to the laser linewidth in a short transmission. Even a low-quality Laser such as the FP laser can be used in a short transmission ($=2$ km) with acceptable penalty (0.22 dB).

Although data sequence is not included in this paper, we can estimate that the power spectrum of the photocurrent will be more broadened when high data rate is employed, since a spectral width of the signal is proportional to data rate . In that case, the data rate may be a more decisive parameter than the linewidths of the laser and the RF oscillator.

4. 64-QAM RADIO OVER FIBER SYSTEMS: EFFECT OF LASER AND RF OSCILLATOR LINEWIDTH ON THE BER PERFORMANCE

4.1. Introduction

The Radio over Fiber(RoF) systems are being considered as a promising solution for the distribution of the radio signal to and from the mobile central office(CO) and the base station (BS) for the modern 3G/4G cellular communication systems. In RoF system unlike conventional systems, the radio signal is sent directly over the fiber channel by modulating the laser diode with it. This technique offers many advantages such as very low loss over the fiber, very high bandwidth of the fiber, centralization of the signal processing functions and the resulting simplicity in the design of the base station[8],[2] . As the signal processing is centralized, the base station contains only a pair of optical to electrical (O/E) and electrical to optical (E/O) converters.

The laser diode and the RF oscillators have finite spectralwidths which cause group delays as the modulated signal travels along the fiber length because of the chromatic dispersion associated with fiber. This phenomenon introduces phase noises in the system. These phase noises affect the system performance severely. The effect of the phase noises on the CNR of the RoF systems have been analyzed by Cho *et al.*[8] in detail. But their focus was mainly on the effect of these phase noises on the CNR penalty of the system and not on the Bit Error Rate (BER) performance which is more effective and practical parameter for comparing the performance of various communication systems.

For QAM systems, this performance degradation becomes even bigger issue since these systems are very sensitive to noise and non linearity induced in optical fiber. In this paper ,we have studied the effects of the laser and RF oscillator spectralwidths upon the BER of the 64-QAM systems. It is observed that the BER degrades rapidly as the laser linewidth

increases and for the laser diodes with linewidths of above 100MHz, BER deteriorates and goes above 10^{-6} . Further, the system BER degrades more rapidly with the RF oscillator linewidth. It is observed that for the RF oscillator's linewidths above 1 Hz, the BER degrades to a value above 10^{-6} which is not acceptable in the design and development of efficient modern communication system. Therefore, a knowledge of the effect of the spectralwidths associated with laser diode and RF oscillators becomes indispensable.

4.2. General Architecture of RoF System

A general architecture of RoF system is given in figure 4.1 below. The data stream modulates the RF carrier, this RF signal and its phase shifted version is then applied at the electrodes of the Dual Electrode- Mach Zehnder Modulator (DE-MZM) to obtain the Optical Single Sideband(OSSB) signal. This externally modulated OSSB signal at the (DE-MZM) output is then transmitted over the Standard Single Mode Fiber (SSMF).

At the receiver end, this signal is detected using a photodiode, filtered ,amplified and then transmitted via the wireless channel to the user terminal. At the user terminal, the received signal is amplified, filtered and demodulated to obtain the data stream. The modulator used is 64-QAM modulator similarly the demodulator at the UT is also 64-QAM demodulator.

The phase noise due to the laser linewidth and the RF oscillator linewidth deteriorates the CNR at the receiver output. This reduced CNR affects the BER performance of the system. Using eqn(), we have the expression for CNR as

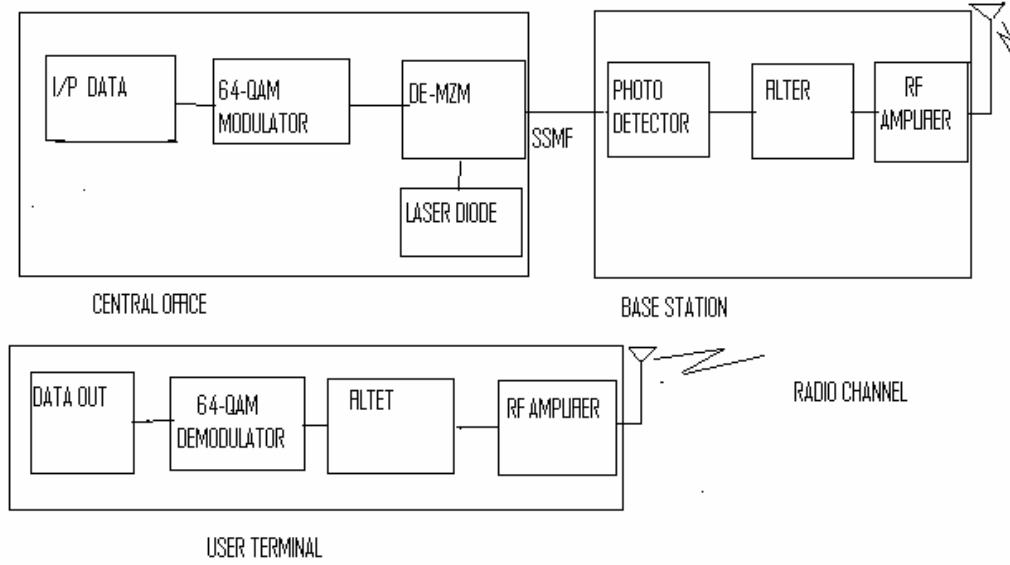


Figure 4.1 General RoF system.

$$CNR = \frac{\mathfrak{R}A^4_1\alpha^2_1p}{N_0 \frac{\gamma_{RF}}{\pi} \cdot \tan\left(\frac{\pi}{2} e^{2\gamma_1\tau_1} p\right)} \quad (4.1)$$

Where

\mathfrak{R} = Photo detector sensitivity

A_1 =constant related to the laser light amplitude A and the losses in fiber .MZM and the joints and splices. given by

$$A_1 = A.L_{MZM}.L_{add}.10^{\frac{-\alpha_{fiber}L_{fiber}}{20}}.J_0(\alpha\pi) \quad (4.2)$$

α_1 =a constant related to the ratio of the first harmonic of the photo detector current to the fundamental component of it, given as

$$\alpha_1 = \frac{\sqrt{2}J_1(\alpha\pi)}{J_0(\alpha\pi)} \quad (4.3)$$

Where $J_n(x)$ denote the Bessel function of the first kind, of order n.and

α =normalized RF voltage given by

$$\alpha = \frac{V_{rf}}{V_{\pi}}$$

Where A is the amplitude of the laser light, L_{MZM} is the loss in the MZM, $L_{add.}$ is the factor accounting for the additional losses in the fiber, α_{fiber} is the loss in the fiber and L_{fiber} is the length of the fiber. V_{rf} is the input RF voltage, and V_{π} is the MZM switching voltage, P is the ratio of the power required for a particular filter used (such as Full width Half Maximum(FWHM) filter etc.) to the total carrier power. This parameter incorporates the effect of the bandwidth of the filter being used. And N_0 is the additive white Gaussian noise(AWGN) power spectral density. The parameters $2\gamma_{LD} = 2\pi\Delta\nu_{LD}$ and $2\gamma_{RF} = 2\pi\Delta\nu_{RF}$, define the angular full-linewidth at half maximum (FWHM) of the Lorentzian shape for the laser and the RF oscillator[2].And $2\gamma_t = 2\pi\Delta\nu_{LD} + \pi\Delta\nu_{RF}$ gives the total linewidth.

$\tau_1 = \tau_1 = \tau + \tau_0$ is the differential delay due to the fiber chromatic dispersion and is given by [3]

$$\tau_1 = D.L_{fiber}.\lambda^2 . \frac{f_{RF}}{c} \quad (4.4)$$

Where D is the fiber chromatic dispersion parameter, L_{fiber} is the fiber length, f_{RF} is the RF frequency and c is the speed of light.

4.3. M-Ary QAM Systems and their BER Performance:

The M-ary QAM technique combines two quadrature components of a continuous wave tone and transmits amplitude and the phase of the carrier signal. The general form of M-ary QAM is defined by the transmitted signal[10]

$$s_i(t) = \sqrt{\frac{2E_0}{T}}a_i.\cos(2\pi fct) + \sqrt{\frac{2E_0}{T}}b_i.\sin(2\pi fct), \quad 0 \leq t \leq T \quad (4.5)$$

Where E_0 is the energy of the signal with the lowest amplitude, and a_i and b_i are a pair of independent integers chosen with the location of the pertinent message point.

The signal $s_i(t)$ consists of two phase quadrature carriers each of which is modulated by a set of discrete amplitudes hence the name Quadrature amplitude modulation.

The signal constellation diagram of the M-Ary QAM is given in following figure.

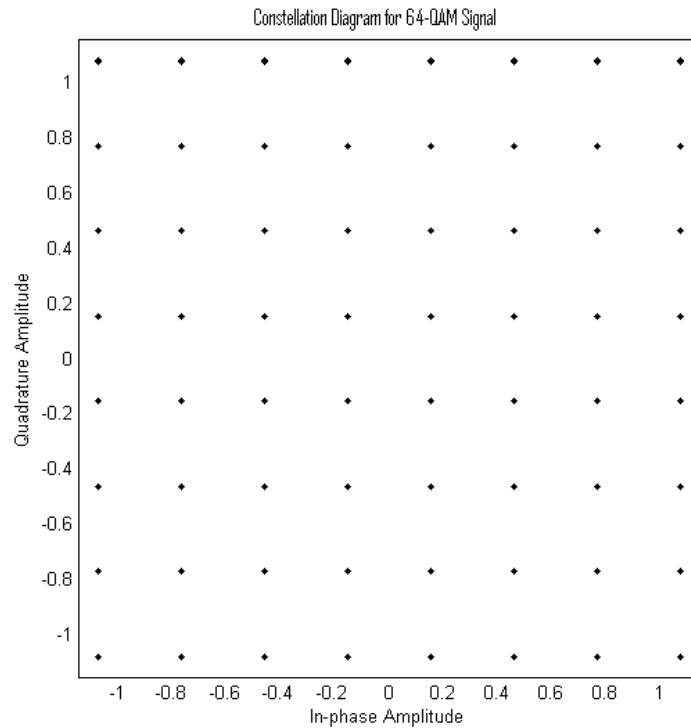


Figure 4.2 Constellation Diagram for 64-QAM

The BER of the QAM system is give in general[2],[10] as

$$Pe = (1 - \frac{1}{\sqrt{M}})erfc(\sqrt{\frac{3CNR}{2(M-1)}}) \quad (4.6)$$

Where

CNR is the carrier to noise ratio at the receiver end.

For 64-ary QAM system, $M=64$ thus the above expression becomes

$$Pe = \frac{7}{8} \operatorname{erfc}\left(\sqrt{\frac{CNR}{42}}\right) \quad (4.7)$$

Now in the above expression for CNR, there are many parameters that need to be evaluated before using this expression to study and simulate the effect of the phase noises on the BER performance of the 64-QAM RoF system.

The first parameter is the photodiode responsivity \mathfrak{R} . For most of the photo diodes its values is between 0.6 to 0.8. Taking the value of R as 0.7 [11]. Now the second constant is A_1 which in tem depend upon other parameters given as

$$\begin{aligned} A_1 &= A.L_{MZM}.L_{add}.10^{\frac{-\alpha_{fiber}L_{fiber}}{20}}.J_0(\alpha\pi) \\ &= V_{rf}/V_{\pi} \end{aligned} \quad 4.8$$

Here L_{MZM} is the loss of the DE- MZM. Now considering the MZM as a integrated waveguide power splitter and combiner, its value can be assumed to be negligible (which is true for small lengths of the waveguide.)

L_{add} is the additional loss caused by the fiber components such as the splices, joints etc. Its value for an 10 Km fiber link can be taken as approximately 3 dB. α_{fiber} is the loss per Km of the fiber and is around .2dB/Km for SSMF. L_{fiber} is the length of the fiber and is equal to 10 Km for this case. α is the modulation index of the MZM and is equal to $\alpha = V_{rf}/V_{\pi}$ Now taking $V_{rf}=1\text{mV}$ and $V_{\pi}=2.2\text{V}$, we obtain $\alpha=.00045$ then the modulation index is given as $\alpha\pi=0.0014$. It gives $J_0(\alpha\pi)$ equal to 1 approximately.

From above all, the value of A_1 is calculated as 0.1342.

N_0 is the power spectral density of the AWGN for very low noise case, it can be taken as 10^{-11} .

Now α_1 depends upon the first harmonic of the of the photo detector and the fundamental component. So the value of α_1 is 0.001

Thus all the constants terms are evaluated, the eqn () is then used to studt the effects of the laser and RF oscillator linewidth on the BER.

5. IMPROVEMENT OF SYSTEM BER

5.1 Introduction

System BER performance of the 64-QAM signals can be improved using channel coding techniques. There are various families of powerful error correcting codes. In this chapter, the effect of the BCH codes is analysed and their effect on the system BER of the 64-QAM systems is demonstrated.

5.2. Bose Chaudhury Hacquenghem (BCH) Codes:

BCH codes are one of the most powerful codes used for the error correction in digital communication systems. These belong to the general family of the codes called the Convolutional codes.

BCH codes use field theory and polynomials over finite fields. To obtain a code over the finite field $GF(q^m)$ its elements are represented as polynomials over the ground field $GF(q)$ modulo some irreducible polynomial. Then a generator polynomial g is chosen. The code words are those polynomials that are the multiple of the generator polynomial.

The lower bounds on the minimum distance of this code can be given if the roots of the generator polynomials have a special form. The BCH code with designed distance δ over the field $GF(q^m)$ is constructed by first finding a polynomial over $GF(q)$ whose roots include δ consecutive powers of γ , some root of unity.

Although the decoding of BCH codes is involved, it can be done efficiently. To detect errors a check polynomial can be constructed so the receiving end can detect if some errors had occurred.

These codes are multiple error correcting codes and a generalization of the

Hamming codes. These are the possible BCH codes⁷ for $m \geq 3$ and $t < 2m-1$:

Block Length: $n = 2m - 1$

Parity Check Bits: $n - k \leq mt$

Minimum distance: $d \geq 2t + 1$

5.3 Code Construction

The codewords are formed by taking the remainder after dividing a polynomial representing our information bits by a generator polynomial. The generator polynomial is selected to give the code its characteristics. All codewords are multiples of the generator polynomial.

Let us turn to the construction of a generator polynomial. It is not simply a minimal, primitive polynomial as in our example where we built GF(16). It is actually a combination of several polynomials corresponding to several powers of a primitive element in GF(2^m).

The discoverers of the BCH codes determined that if α is a primitive element of GF(2^m), the generator polynomial is the polynomial of lowest degree over GF(2) with $\alpha, \alpha^2, \alpha^3, \dots, \alpha^{2t}$ as roots. The length of a codeword is $2m - 1$ and t is the number of correctable errors. Lin concludes⁸ that the generator is the least common multiple of the minimal polynomials of each α^i term. A simplification is possible because every even power of a primitive element has the same minimal polynomial as some odd power of the element, halving the number of factors in the polynomial.

$$\text{Then } g(x) = \text{lcm}(m_1(x), m_3(x), \dots, m_{2t-1}(x)). \quad 5.1$$

These BCH codes are called primitive because they are built using a primitive element of GF(2^m). BCH codes can be built using nonprimitive elements, too, but the block length is typically less than $2m - 1$.

As an example, let us construct a generator polynomial for BCH(31,16). Such a codeword structure would be useful in simple remote control applications where the information transmitted consists of a device identification number and a few control bits, such as “open door” or “start ignition.”

This code has 31 codeword bits, 15 check bits, corrects three errors ($t = 3$), and has a minimum distance between codewords of 7 bits or more. Therefore, at first glance we need $2t - 1 = 5$ minimal polynomials of the first five powers of a primitive element in minimal polynomials, so we only use the first three minimal polynomials corresponding to odd powers of the GF(32). But the even powers’ minimal polynomials are duplicates of odd powers’ primitive element.

The field we are working in is GF(32), shown below. This was generated using primitive polynomial $x^5 + x^2 + 1$ over GF(32)

We need first a primitive element. Well, α is a primitive element in GF(32). Next we need the minimal polynomials of the first three odd powers of α . Tables of minimal polynomials appear in most texts on error control coding. Lin and Costello, Pless, and Rorabaugh⁹ exhibit algorithms for finding them using cyclotomic cosets. From Lin and Costello¹⁰, the first three odd power of α minimal polynomials are:

$$\alpha: m_1(x) = x^5 + x^2 + 1 \tag{5.2}$$

$$\alpha^3: m_3(x) = x^5 + x^4 + x^3 + x^2 + 1 \tag{5.3}$$

$$\alpha^5: m_5(x) = x^5 + x^4 + x^2 + x + 1 \tag{5.4}$$

Therefore, $g(x) = \text{lcm}(m_1(x), m_3(x), m_5(x)) = m_1(x) m_3(x) m_5(x)$ (since these are irreducible).

$$\text{So } g(x) = (x^5 + x^2 + 1)(x^5 + x^4 + x^3 + x^2 + 1)(x^5 + x^4 + x^2 + x + 1) = x^{15} + x^{11} + x^{10} + x^9 + x^8 + x^7 + x^5 + x^3 + x^2 + x + 1. \tag{5.5}$$

Field of 32 elements generated by $x^5 + x^2 + 1$		
Power Form	n-Tuple Form	Polynomial Form
0	00000	0
1	00001	1
α	00010	α
α^2	00100	α^2
α^3	01000	α^3
α^4	10000	α^4
α^5	00101	$\alpha^2 + 1$
α^6	01010	$\alpha^3 + \alpha$
α^7	10100	$\alpha^4 + \alpha^2$
α^8	01101	$\alpha^3 + \alpha^2 + 1$
α^9	11010	$\alpha^4 + \alpha^3 + \alpha$
α^{10}	10001	$\alpha^4 + 1$
α^{11}	00111	$\alpha^2 + \alpha + 1$
α^{12}	01110	$\alpha^3 + \alpha^2 + \alpha$
α^{13}	11100	$\alpha^4 + \alpha^3 + \alpha^2$
α^{14}	11101	$\alpha^4 + \alpha^3 + \alpha^2 + 1$
α^{15}	11111	$\alpha^4 + \alpha^3 + \alpha^2 + \alpha + 1$
α^{16}	11011	$\alpha^4 + \alpha^3 + \alpha + 1$
α^{17}	10011	$\alpha^4 + \alpha + 1$
α^{18}	00011	$\alpha + 1$
α^{19}	00110	$\alpha^2 + \alpha$
α^{20}	01100	$\alpha^3 + \alpha^2$
α^{21}	11000	$\alpha^4 + \alpha^3$
α^{22}	10101	$\alpha^4 + \alpha^2 + 1$
α^{23}	01111	$\alpha^3 + \alpha^2 + \alpha + 1$
α^{24}	11110	$\alpha^4 + \alpha^3 + \alpha^2 + \alpha$
α^{25}	11001	$\alpha^4 + \alpha^3 + 1$
α^{26}	10111	$\alpha^4 + \alpha^2 + \alpha + 1$
α^{27}	01011	$\alpha^3 + \alpha + 1$
α^{28}	10110	$\alpha^4 + \alpha^2 + \alpha$
α^{29}	01001	$\alpha^3 + 1$
α^{30}	10010	$\alpha^4 + \alpha$

Table 5.1 Field of 32 elements generated by polynomial.

To encode a block of bits, let us first select as our information the binary word 1000001 for the letter “A” and call it $f(x)$, placing it in the 16-bit information field . Next, we append a number of zeros equal to the degree of the generator polynomial (fifteen in this

case). This is the same as multiplying $f(x)$ by x^{15} . Then we divide by the generator polynomial using binary arithmetic (information bits are bold):

```

-----
1000111110101111)00000000010000010000000000000000
1000111110101111
-----
1101101011110000
1000111110101111
-----
1010101010111110

```

The remainder is zero if there are no errors. This makes sense because we computed the checkbits ($r(x)$) from the information bits ($f(x)$) in the following way:

$$f(x) x^n = q(x) g(x) + r(x) \quad 5.6$$

The operation $f(x) x^n$ merely shifts $f(x)$ left n places. Concatenating the information bits $f(x)$ with the checkbits $r(x)$ and dividing by $g(x)$ again results in a remainder, $r'(x)$, of zero as expected because

$$f(x) x^n + r(x) = q(x) g(x) + r'(x) \quad 5.7$$

If there are errors in the received codeword, the remainder, $r'(x)$, is nonzero, assuming that the errors have not transformed the received codeword into another valid codeword. The remainder is called the syndrome and is used in further algorithms to actually locate the errant bits and correct them, but that is not a trivial matter.

The BCH codes are also cyclic, and that means that any cyclic shift of our example codeword is also a valid codeword. For example, we could interchange the information and checkbits fields in the last division above (a cyclic shift of 15 bits) and the remainder would still be zero.

5.4 Decoding the BCH Code

Determining where the errors are in a received codeword is a rather complicated process.

Decoding involves three steps:

1. Compute the syndrome from the received codeword.
2. Find the error location polynomial from a set of equations derived from the syndrome.
3. Use the error location polynomial to identify errant bits and correct them.

We have seen that computing the syndrome is not difficult. However, with the BCH codes, to implement error correction we must compute several components which together comprise a syndrome vector. For a t error correcting code, there are $2t$ components in the vector, or six for our triple error correcting code. These are each formed easily using polynomial division, as above, however the divisor is the minimal polynomial of each successive power of the generating element, α .

Let $v(x)$ be our received codeword. Then $S_i = v(x) \bmod m_i(x)$, where $m_i(x)$ is the minimal polynomial of α^i . In our example,

$$S_1(x) = v(x) \bmod m_1(x) \quad 5.8$$

$$S_2(x) = v(x) \bmod m_2(x) \quad 5.9$$

$$S_3(x) = v(x) \bmod m_3(x) \quad 5.10$$

$$S_4(x) = v(x) \bmod m_4(x) \quad 5.11$$

$$S_5(x) = v(x) \bmod m_5(x) \quad 5.12$$

$$S_6(x) = v(x) \bmod m_6(x) \quad 5.13$$

Now in selecting the minimal polynomials, we take advantage of that property of field elements whereby several powers of the generating element have the same minimal polynomial. If $f(x)$ is a polynomial over $GF(2)$ and α is an element of $GF(2^m)$, then if $b = 2^i \alpha$ is also a root of $f(x)$ for $i \geq 0$ 13. These are called conjugate elements. From this we see that all powers of α such as $\alpha^2, \alpha^4, \alpha^8, \alpha^{16}, \dots$ are roots of the minimal polynomial of α . In $GF(32)$ which applies to our example, we must find the minimal polynomials for α through α^6 . The six minimal polynomials are:

$$m_1(x) = m_2(x) = m_4(x) = x^5 + x^2 + 1 \quad 5.14$$

$$m_3(x) = m_6(x) = x^5 + x^4 + x^3 + x^2 + 1 \quad 5.14$$

$$m_5(x) = x^5 + x^4 + x^2 + x + 1 \quad 5.15$$

Next, we form a system of equations in α :

$$S1(\alpha) = \alpha + \alpha^2 + \dots + \alpha^n \quad 5.16$$

$$S2(\alpha^2) = (\alpha)^2 + (\alpha^2)^2 + \dots + (\alpha^n)^2 \quad 5.17$$

$$S3(\alpha^3) = (\alpha)^3 + (\alpha^2)^3 + \dots + (\alpha^n)^3 \quad 5.18$$

$$S4(\alpha^4) = (\alpha)^4 + (\alpha^2)^4 + \dots + (\alpha^n)^4 \quad 5.19$$

$$S5(\alpha^5) = (\alpha)^5 + (\alpha^2)^5 + \dots + (\alpha^n)^5 \quad 5.20$$

$$S6(\alpha^6) = (\alpha)^6 + (\alpha^2)^6 + \dots + (\alpha^n)^6 \quad 5.21$$

It turns out that each syndrome equation is a function only of the errors in the received codeword. The α_i are the unknowns, and a solution to these equations yields information we use to construct an error locator polynomial. One can see that this system is underconstrained, there being multiple solutions. The one we are looking for is the one that indicates the minimum number of errors in the received codeword (we are being optimistic).

First, make a table (using BCH(31,16))

μ	$\sigma^{(\mu)}(x)$	d_μ	l_μ	$2\mu - l_\mu$
$-\frac{1}{2}$	1	1	0	-1
0	1	S_1	0	0
1				
2				
$t = 3$				

Table 5.2 Decoding of BCH code

The BCH decoding algorithm follows.

1. Initialize the table as above. Set $\mu = 0$.
2. If $d_\mu = 0$, then $\sigma(\mu + 1)(x) = \sigma(\mu)(x)$. Let $L = l_\mu + 1$.
3. If $d_\mu \neq 0$, then find a preceding row (row ρ) with the most positive $2\mu - l_\mu$ and $d_\rho \neq 0$. Then

$$\sigma(\mu + 1)(x) = \sigma(\mu)(x) + d_\mu d_\rho^{-1} x^{2(\mu - \rho)} \sigma(\rho)(x)$$
. If $\mu = t - 1$, terminate the algorithm.
4. $l_{\mu + 1} = \deg(\sigma(\mu + 1)(x))$.

5. $d_{\mu+1} = S^{2\mu+3} + \sigma_1$
 $(\mu+1) S^{2\mu+2} + \sigma_2$
 $(\mu+1) S^{2\mu+1} + \dots + \sigma_L$
 $(\mu+1) S^{2\mu+3} - L$. σ_i is the coefficient of
the i -th term in $\sigma(x)$.
6. Increment μ and repeat from step 2.

At each step we are computing the next approximation to the error locator polynomial $\sigma(\mu)(x)$.

Depending upon the result of the previous step, we may be required to add a correction term, d_{μ} . To $\sigma(\mu)(x)$. When we have completed step $t-1$, $\sigma(\mu)(x)$ is the final error locator polynomial if it has degree less than or equal to t . If the degree is greater than t , then the codeword cannot be corrected (there are more than t errors).

Let us work out an example. Given our sample codeword (0000000001000001100101000100010)

we introduce three errors as if it were a corrupt received codeword,

$v(x) = 0001000011000001100100000100010$. Now we set to work computing syndrome components. Remember that the check polynomials are, with their binary equivalents,

$$m_1(x) = m_2(x) = m_4(x) = x^5 + x^2 + 1 \text{ (100101)}, \quad 5.22$$

$$m_3(x) = m_6(x) = x^5 + x^4 + x^3 + x^2 + 1 \text{ (111101)}, \quad 5.23$$

$$m_5(x) = x^5 + x^4 + x^2 + x + 1 \text{ (110111)}, \quad 5.24$$

so we have three divisions to do to find six syndrome components. These are done by simple binary division, as above, details omitted.

$$S_1(x) = v(x) \bmod m_1(x) = x^2 \quad 5.25$$

$$S_2(x) = v(x) \bmod m_2(x) = x^2 \quad 5.26$$

$$S_3(x) = v(x) \bmod m_3(x) = x^4 + x^3 + x + 1 \quad 5.27$$

$$S_4(x) = v(x) \bmod m_4(x) = x^2 \quad 5.28$$

$$S_5(x) = v(x) \bmod m_5(x) = x^4 + x$$

$$S_6(x) = v(x) \bmod m_6(x) = x^4 + x^3 + x + 1$$

We find $S_i(\alpha_i)$ by substituting α_i into the equations above, reducing using the table we derived for GF(32) when necessary. Remember that $\alpha^5 = \alpha^2 + 1$.

$$S1(\alpha) = \alpha^2 \quad 5.29$$

$$S2(\alpha^2) = \alpha^4 \quad 5.30$$

$$S3(\alpha^3) = (\alpha^3)^4 + (\alpha^3)^3 + (\alpha^3) + 1 = \alpha^{14} \quad 5.31$$

$$S4(\alpha^4) = \alpha^8 \quad 5.32$$

$$S5(\alpha^5) = (\alpha^5)^4 + (\alpha^5) = \alpha^{29} \quad 5.33$$

$$S6(\alpha^6) = (\alpha^6)^4 + (\alpha^6)^3 + (\alpha^6) + 1 = \alpha^{28} \quad 5.34$$

The final error locator polynomial is $\sigma(\mu)(x) = \alpha^{27}x^3 + \alpha^{11}x^2 + \alpha^2x + 1$.

We next find the roots of $\sigma(\mu)(x)$ in GF(32) by trial and error substitution. (There is a search algorithm due to Chen that is more efficient.) The roots are α^4 , α^9 , and α^{22} . The bit positions of the error locations correspond to the inverses of these roots, or α^{27} , α^{22} , and α^9 , respectively. A polynomial corresponding to the error pattern would then be $e(x) = x^{27} + x^{22} + x^9$. Adding $e(x)$ to the received codeword corrects the errors. Examining the original corrupt codeword we created,

$$\begin{aligned} v(x) &= 0001000011000001100100000100010 \\ \oplus e(x) &= 0001000010000000000001000000000 \end{aligned}$$

$$c(x) = 0000000001000001100101000100010$$

and it is clear that the calculated error pattern matches the actual error pattern and $c(x)$ matches our original codeword.

If there are no errors, then the syndromes all work out to zero. One to three errors produce the corresponding number of bits in $e(x)$. More than three errors typically results in an error locator polynomial of degree greater than $t = 3$. However, it is again possible that seven bit errors could occur, resulting in a zero syndrome and a false conclusion that the message is correct. That is why most error correction systems take other steps to ensure data integrity, such as using an overall check code on the entire sequence of code words comprising a message.

In practice, error correction is done in either software or hardware. The Berlekamp algorithm is complex and not too attractive when considered for high-speed communications systems, or operation on power limited microprocessors.

6. RESULTS

The BER is studied with the laser linewidth, RF oscillator linewidth and the filter bandwidth dependent parameter p . The following figures show the variation of the BER with these parameters.

6.1 UNCODED SYSTEMS

6.1.1. EFFECT OF THE LASER LINEWIDTH:

The variation of the BER with the laser linewidth is shown in figure below. The BER is plotted against the laser linewidth for three different values of the RF oscillator linewidth i.e 0.8 Hz, 0 Hz and 1.2 Hz. As can be seen, the BER increases monotonously with the increase in the laser linewidth and as we increase the values of the RF oscillator linewidth, the performance deteriorates further. If we take BER of 10^{-6} as minimum BER to support any quality communication over the channel, then as can be seen in the figure, for RF oscillator linewidth of 1 Hz, laser diodes of up to 100 MHz linewidth can sustain a quality communication over the channel. As the RF oscillator linewidth is decreased to 0.8 Hz, this limit extends up to 580 MHz for line width of laser diode. Thus, by decreasing the RF oscillator linewidth, we can achieve the same value of BER at relatively higher values of laser linewidths. For RF oscillator linewidth of 1.2 Hz, the link fails to support quality communication for laser linewidths as low as few Mega Hertz's. Thus there is a tradeoff between the RF oscillator linewidth and the laser line width deployed in RoF system. If we design the link with the cheaper laser diodes with comparatively larger linewidths, then we have to use the much more stable RF oscillators with linewidths much lower than 1Hz.

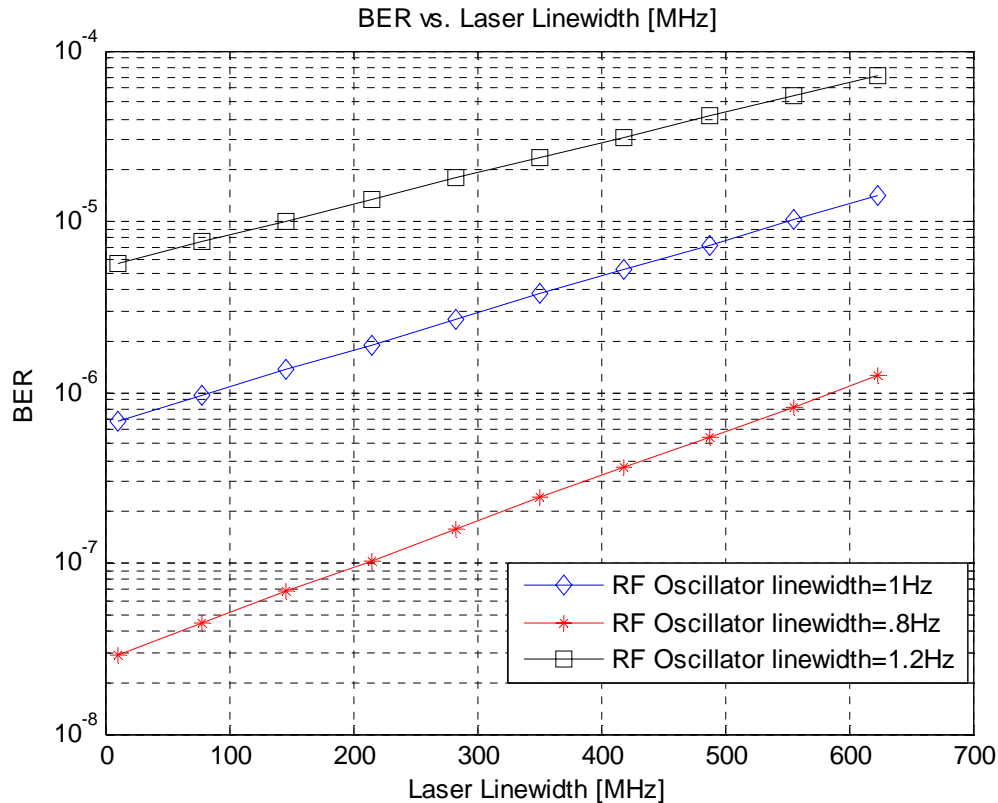


Figure 6.1 BER vs. laser linewidth (MHz) for different RF oscillator line width

6.1.2 EFFECT OF THE PARAMETER p :

The effect of the filter bandwidth dependent factor p on the BER of the system is shown in the figure 3. Here the BER is plotted against the parameter p for three different values of laser linewidth viz. 10 MHz, 100 MHz, 300 MHz, and the RF oscillator linewidth is assumed to be 1 Hz. As can be seen in the figure, the BER increases steeply when p is varied from 0 to 1. At laser linewidth of 10 MHz, the BER goes above 10^{-6} when p is around 0.55. And for the 99% bandwidth filter, the BER increases beyond 10^{-2} . Thus there is a compromise between the filter bandwidth and the BER; greater the filter bandwidth, the higher the system BER. Also as is evident from the figure, here the parameter p is more decisive factor than the laser linewidth. The BER does not change significantly as the laser linewidth is varied from 10 MHz to 300 MHz.

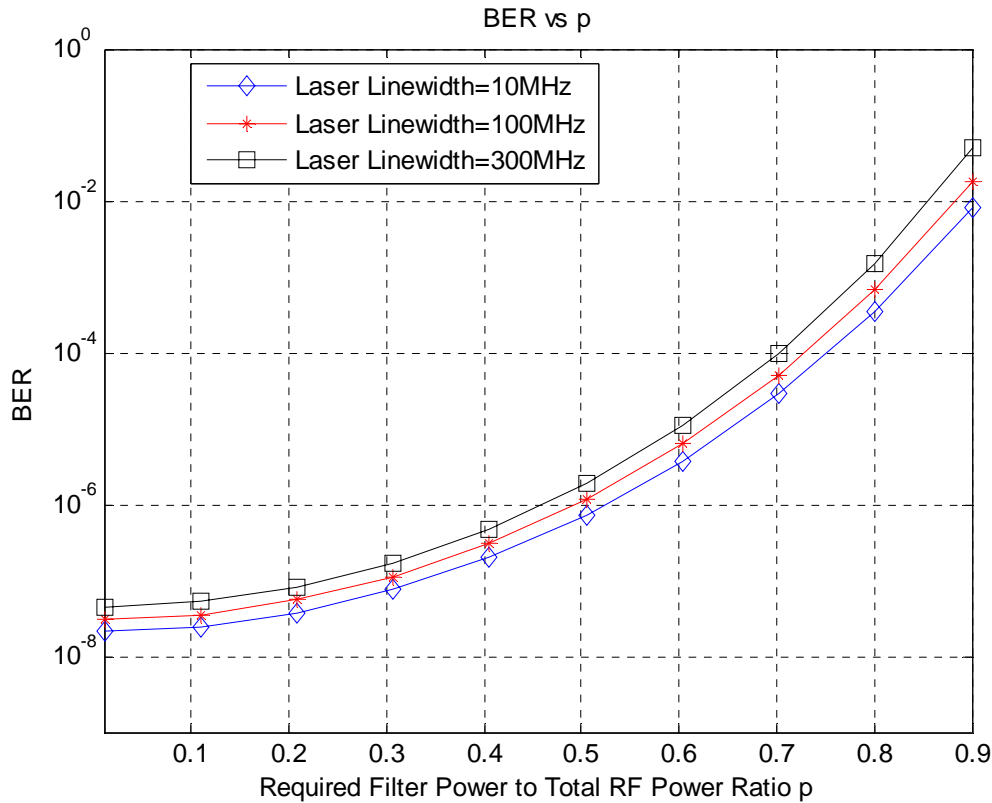


Figure 6.2 BER vs. p for different laser line width

6.1.3 EFFECT OF THE RF OSCILLATOR LINEWIDTH:

The variation of the BER with the RF oscillator linewidth is shown in the figure6.3. and figure6.4. The BER is plotted against the RF oscillator linewidth for three different values of the laser linewidth viz. 10MHz,150 MHz and 300MHz. BER increases monotonously as we increase the RF oscillator linewidth from 0 to 10 Hz. As can be seen in the figure, for the RF oscillator linewidths above 1 Hz, BER degrades very badly, rising above 10^{-6} . It is also evident from the figure that the effect of the RF oscillator linewidth is more pronounced than that of the laser linewidth for the short haul RoF links. There is not much variation in the BER as the laser linewidth is varied from 10 to 300 MHz. Thus RF oscillator linewidths should be maintained below 1Hz for satisfactory performance of the link.

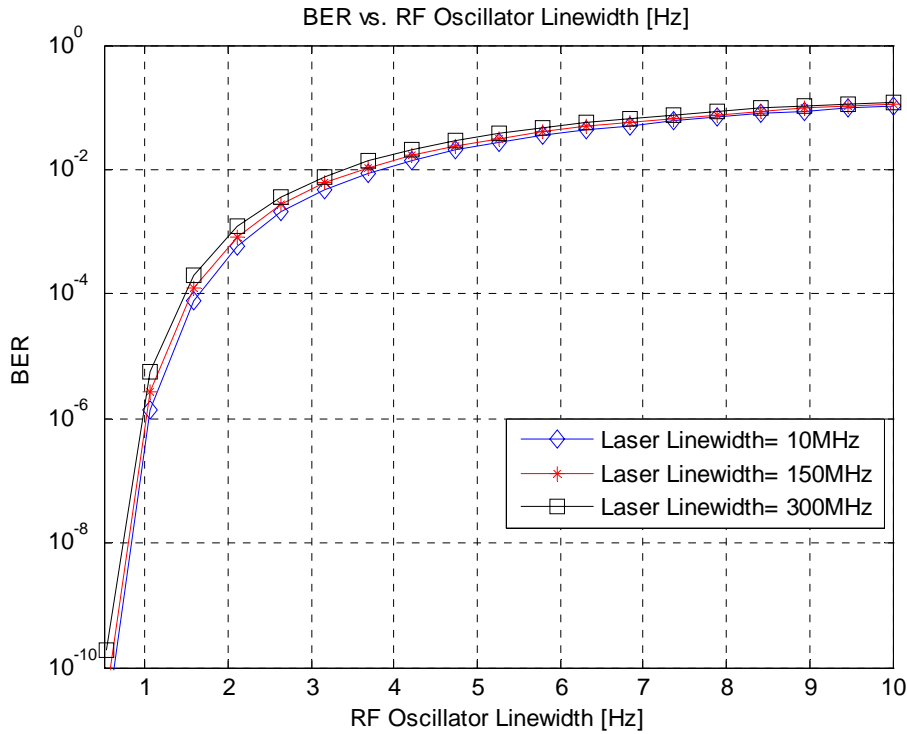


Figure 6.4 BER vs. RF oscillator linewidth [Hz].

We can also observe from the figure 6.4, where the effects of RF oscillator linewidth is plotted at different values of p , that the effect of Bandwidth is also equally pronounced. And we have to make a considerable trade of between the bandwidth requirement and the RF oscillator linewidth. As can be seen that the BER deteriorates rapidly as value of p is increased. And for values of p above 0.8, there is hardly any meaningful communication possible in the channel for the RF oscillator linewidths of above 1 Hz. Thus we need to employ highly stable local oscillators to if higher bandwidths are required. Which poses a lot of design issues.

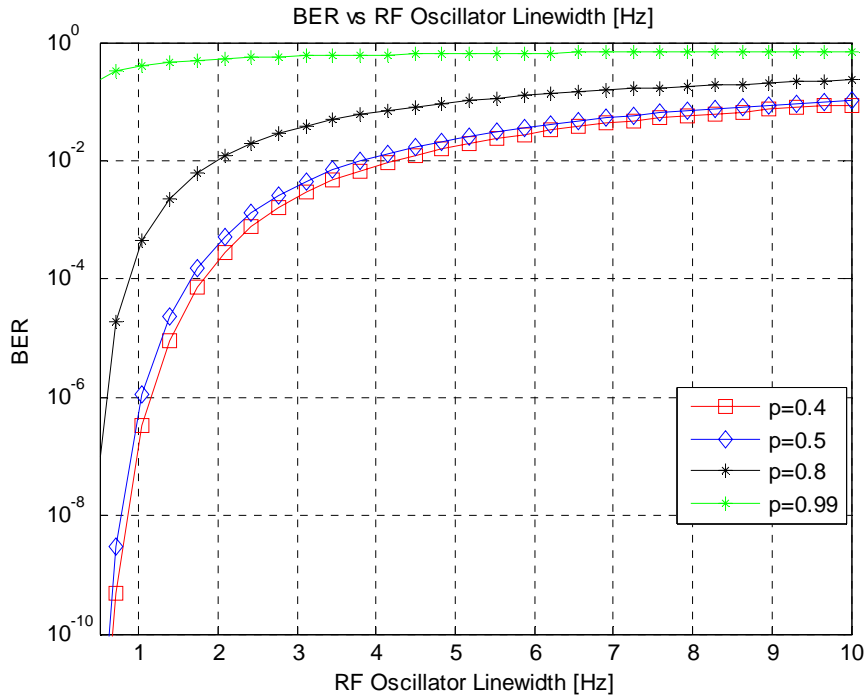


Figure 6.3 BER vs. RF oscillator linewidth [Hz] for different values of p.

6.2. EFFECT OF CHANNEL CODING:

The channel coding considerably improves the system BER. As is analyzed in the following graphs, the Systems BER can be Brought to as low as 10^{-14} theoretically.

In the first figure below, as can be seen, channel coding decreases the system BER from 10^{-7} to around 10^{-12} for low Laser linewidths few tens of megahertz's. For higher linewidths too, the BER barely goes above 10^{-10} , at RF oscillator linewidths of 0.8 Hz. For RF oscillator linewidth of 1 Hz, BER still remains in the interval of 10^{-11} to 10^{-12} for the entire range of the laser linewidth. Thus for these cases we can use cheaper diodes and still get satisfactory system performance. Which will reduce the system cost considerably, since the Laser diodes with smaller spectral widths are more expensive and more difficult to fabricate. As For the case where RF Oscillator linewidth is 1.2 Hz, BER remains between 10^{-9} and 10^{-9} . Noting that the minimum system BER should be atleast 10^{-6} , it can be seen that for this case also system gives satisfactory performance for whole spectrum of the laser diodes.

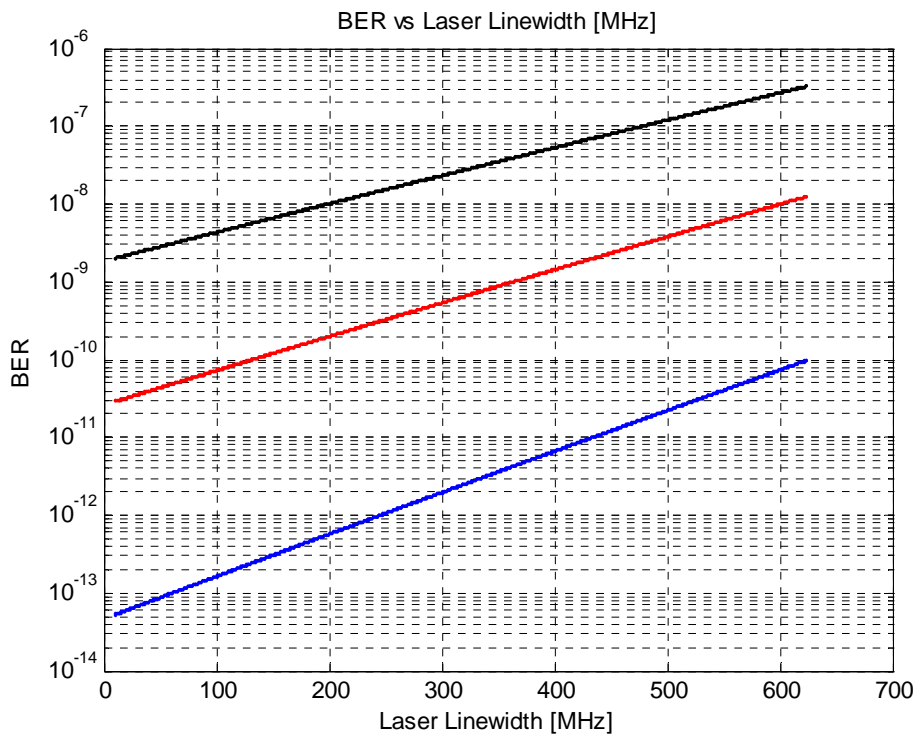


Figure 6.4 BER versus Laser Linewidth {MHz} for coded case.

In the second graph below, the effect of the channel coding is explored for the case of the filter bandwidth dependent parameter p . As seen in this case, there is a significant decrease in the system BER. For the case of 10 MHz laser diode, we see that the BER lies between 10^{-14} to 10^{-6} against the uncoded case where it lies between 10^{-8} to 10^{-2} or less for the entire range of p .

Also it is evident that as laser diode linewidth is increased, BER rises to 10^{-12} which still is significantly less than the uncoded case. So even at worst case, the BER for the half power bandwidth filter is considerably less than 10^{-6} .

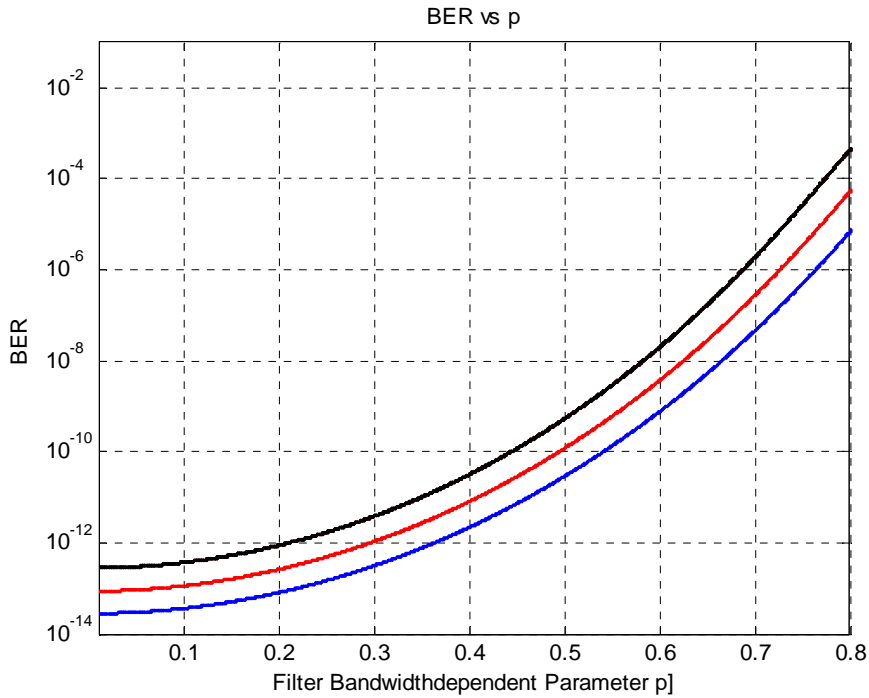


Figure 6.5 BER versus Filter bandwidth dependent parameter p for coded case.

In the third graph the effect of the coding is shown on the BER versus RF oscillator linewidth curve. In this case also the effect is evident. It can be clearly seen that BER remains below 10^{-6} for RF oscillator linewidths as high as around 1.5- 1.8 Hz against the uncoded case where the 10^{-6} value is crossed at around 1.0 Hz.

Its evident from the above results that the channel coding is an effective way to reduce the system BER. Thus even if the effects of the RF oscillator and the laser diode linewidths are not compensated properly. Thus Use of the BCH codes can reduce the system cost considerably.

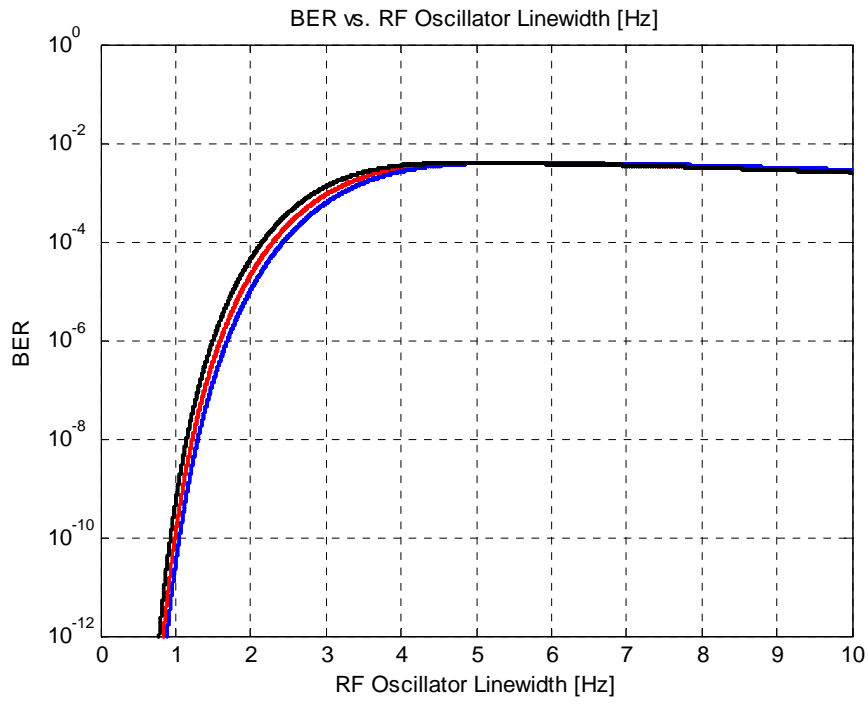


Figure6.6 BER versus RF Oscillator Linewidth [Hz] for coded case

CONCLUSION

We have studied effect of the phase noises induced from the laser linewidth and the RF oscillator linewidth on the BER of the 64-Ary QAM Radio over fiber systems.

In most of the fiber communication systems, the lower threshold for the BER is less than 10^{-6} . If the BER increases above this value, the link will not be able to support the present day high quality multimedia services offered by the cellular operators. Also the phase noises limit the bandwidth of the system. Greater the bandwidth of the filter, the more the noise into the system and hence poorer the BER. The BER falls to the 10^{-6} level for 55% bandwidth filter. For 99% bandwidth filter, the BER falls even below 10^{-2} . Thus we have to make a compromise between the filter bandwidth and the BER.

The effect of the RF oscillator linewidth on the system BER is also studied. For the oscillator linewidths above 1.0 Hz, system BER falls below 10^{-6} . Thus for a better BER performance, we have to restrict the oscillator linewidth below 1.0 Hz. This means we need to use highly stable RF oscillators for this purpose. For oscillator linewidths above this, the BER performance deteriorate very rapidly. Further, it is evident from the above discussion that for RoF links, the effect of the RF oscillator linewidth on the system BER is more pronounced than that of the laser line width.

Also there is a trade off between the bandwidth dependent parameter p and the RF oscillator linewidth. As is evident from the discussion above in section 6.1.3, the BER performance of the system employing 80% or above bandwidth filter, is abysmally low. And for values of p above .9, there is almost no communication possible over the channel for the RF oscillator linewidths of above 1 Hz. Thus in such cases, it is required to use Highly stable local oscillators that have the linewidths of below 1 Hz. The use of Such oscillators is bound the increase the system cost.

LIST OF ABBREVIATIONS

FTTA	Fiber To The Air
BS	Base Station
CS	Central Station
O/E	Optical to Electrical
E/O	Electrical to Optical
QPSK	Quadrature Phase Shift Keying
QAM	Quadrature Amplitude Modulation
RoF	Radio over Fiber
RF	Radio Frequency
IF	Intermediate Frequency
CO	Central Office
UT	User Terminal
PD	Photo Detector
RIN	Relative Intensity Noise
DR	Dynamic Range
SNR	Signal To Noise Ratio
MA	Multiple Access
TDMA	Time Division Multiple Access
WDM	Wavelength Division Multiplexing
CDMA	Time Division Multiple Access
RAU	Remote Antenna Unit
CMOS	Complementary Metal Oxide Semiconductor
FTTP	Fiber To The Premises
FTTH	Fiber To The Home
FTTC	Fiber To The Cabinet
FTTB	Fiber To The Building
ADSL	Asynchronous Digital Subscriber Line
FWA	Fiber Wireless Access

PON	Passive Optical Network
LAN	Local Area Network
OFDM	Orthogonal Frequency Division Multiplexing
DFB-LD	Distributed FeedBack Laser Diode
WiBro	Wireless Broadband
3G	Third Generation
4G	Fourth Generation
WLAN	Wireless Local Area Network
B3G	Beyond third Generation
IMD	Inter Modulation Distortion
RVC	Road Vehicle Communication
IVC	Inter Vehicle Communication
ITS	Intellegent Transport System
DAS	Distributed Antenna System
ODSB	Optical Double SideBand
OSSB	Optical Single SideBand
DE-MZM	Dual-Electrode Mach Zehnder Modulator
BER	Bit Error Rate
PSD	Power Spectral Density
CNR	Carrier to Noise Ratio
BCH	Bose Chaudhury Hacquenghem
LO	Local Oscillator

7. REFERENCES:

1. P. Daino, P. Spano, M. Tamburrini, and S. Piazzolla, "Phase noise and spectral lineshape in semiconductor lasers," *IEEE J. Quantum Electron.*, vol. QE-19, p. 266, 1983
2. H. Al-Raweshidy, *Radio Over Fiber Technologies for Mobile Communications Networks*. Boston, MA: Artech House, 2002.
3. Y. Yamamoto, T. Mukai, and S. Saito, "Quantum phase noise and linewidth of a semiconductor laser," *Electron. Lett.*, vol. 17, p. 327, 1981.
4. C. H. Henry, "Theory of the linewidth of semiconductor lasers," *IEEE J. Quantum Electron.*, vol. QE-18, p. 259, 1982
5. B. Sklar, *Digital Communications*. Englewood Cliffs, NJ: Prentice-Hall, 1988, pp. 43–44.
6. K.-I. Kitayama, "Ultimate performance of optical DSB signal-based millimeter-wave fiber-radio system: Effect of laser phase noise," *J. Lightw. Technol.*, vol. 17, no. 10, pp. 1774–1781, Oct. 1999.
7. U. Gliese, "Chromatic dispersion in fiber-optic microwave and millimeter-wave links," *IEEE Trans. Microw. Theory Tech.*, vol. 44, no. 10, pp. 1716–1724, Oct. 1996.
8. Cho.T.S.,Yun.C,Song.J.I,Kim.K. "Analysis of CNR Penalty of Radio-Over-Fiber Systems Including the Effects of Phase Noise From Laser and RF Oscillator", *JLT Vol. 23, No. 12*, pp. 4093-4100, December 2005
9. G. P. Agrawal, *Fiber-Optic Communication Systems*. New York: Wiley, 1997.
10. B.P. Lathi, *Modern Digital and Analog Communication System*, HRW, Philadelphia, 1989.
11. D. Novak, "The merging of the wireless and fiberoptic worlds," in *CLEO Tech. Dig.*, 2002, p. 276. Paper CTuS1.
12. M. Bibey, F. Deborgies, M. Krakowski, and D. Mongardien, "Very low phase-noise optical links-experiments and theory," *IEEE Trans. Microw. Theory Tech.*, vol. 47, no. 12, pp. 2257–2261, Dec. 1999.
13. W. P. Robins, *Phase Noise in Signal Sources*. London, U.K.: Peter Peregrinus, 1982, pp. 77–78.

14. M. Bibey, F. Deborgies, M. Krakowski, and D. Mongardien, "Very low phase-noise optical links-experiments and theory," *IEEE Trans. Microw. Theory Tech.*, vol. 47, no. 12, pp. 2257–2261, Dec. 1999.
15. W. Shieh and L. Maleki, "Phase noise of optical interference in photonic RF systems," *IEEE Photon. Tech. Lett.*, vol. 10, no. 11, pp. 1617–1619, Nov. 1998.
16. H. Harada, K. Sato and M. Fujise, "A Radio-on-Fiber Based Millimeter-Wave Road-Vehicle Communication System by a Code Division Multiplexing Radio Transmission Scheme," *IEEE Trans. Intelligent Transport. Sys.*, vol. 2, no. 4, pp. 165-179, Dec. 2001.
17. K. Kitayama, "Architectural considerations of radio-on-fiber millimeter-wave wireless access systems," *Signals, Systems, and Electron., 1998 URSI International Symposium*, pp. 378-383, 1998.
18. D. Novak, Z. Ahmed, R. B. Waterhouse, and R. S. Tucker, "Signal generation using pulsed semiconductor lasers for application in millimeter-wave wireless links," *IEEE Trans. Microwave Theory Tech.*, vol. 43, pp. 2257-2262, 1995.
19. T. Kuri, K. Kitayama, and Y. Ogawa, "Fiber-Optic Millimeter-Wave Uplink System Incorporating Remotely Fed 60-GHz-Band Optical Pilot Tone," *IEEE Trans. Microwave Theory Tech.*, vol. 47, no. 7, pp. 1332-1337, Jul. 1999.
20. K. J. Williams, and R. D. Esman, "Optically Amplified Downconverting Link with Shot-Noise-Limited Performance," *IEEE Photon. Technol. Lett.*, vol. 8, no. 1, pp. 148-150, Jan. 1996.
21. L. Noël, D. Wake, D. G. Moodie, D. D. Marcenac, L. D. Westbrook, and D. Nasset, "Novel Techniques for High-Capacity 60-GHz Fiber-Radio Transmission Systems," *IEEE Trans. Microwave Theory Tech.*, vol. 45, no. 8, pp. 1416-1423, Aug. 1997.